EURADOS
European Radiation Dosimetry Group e. V.

EURADOS Report 2013-02

Braunschweig, May 2013

High-energy quasi-monoenergetic neutron fields: existing facilities and future needs

Pomp S., Bartlett D.T., Mayer S., Reitz G., Röttger S., Silari, M., Smit F.D., Vincke H., and Yasuda H.

ISSN 2226-8057

ISBN 978-3-943701-04-3

European Radiation Dosimetry Group e. V.

EURADOS-2013-02

Braunschweig, May 2013

High-energy quasi-monoenergetic neutron fields: existing facilities and future needs

Pomp S.[1], Bartlett D.T.[2], Mayer S.[3], Reitz G.[4], Röttger S.[5], Silari, M.[6], Smit F.D.[7], Vincke H.[6], and Yasuda H.[8]

[1]Uppsala University, Uppsala, Sweden

[2]Abingdon, Oxfordshire, United Kingdom

[3]Paul Scherrer Institute, Villigen, Switzerland

[4]Deutsches Zentrum für Luft-und Raumfahrt, Cologne, Germany

[5]Physikalisch-Technische Bundesanstalt, Braunschweig, Germany

[6]CERN, Geneva, Switzerland

[7]iThemba Laboratory for Accelerator Based Sciences, Somerset West 7129, South Africa

[8]UNSCEAR Secretariat, Vienna, Austria

ISSN 2226-8057

ISBN 978-3-943701-04-3

Imprint

Issued by:
European Radiation Dosimetry e. V.
Bundesallee 100
38116 Braunschweig
Germany
office@eurados.org
www.eurados.org

The European Radiation Dosimetry e.V. is a non-profit organization promoting research and development and European cooperation in the field of the dosimetry of ionizing radiation. It is registered in the Register of Associations (Amtsgericht Braunschweig, registry number VR 200387) and certified to be of non-profit character (Finanzamt Braunschweig-Altewiekring, notification from 2008-03-03).

Liability Disclaimer

Content:

Abstract

High-energy neutrons are the dominant component of the prompt radiation field present outside the shielding of high-energy accelerators, and are a significant component of the cosmic radiation fields in aircraft and in spacecraft. In radiotherapy using high-energy medical accelerators, high-energy neutrons are a secondary component of the fields in the beam delivery system and in the patient's body. The range of neutron energies in these fields extends from thermal energies to several GeV, and the energy distributions of energy fluence generally have several regions of greater intensity: at thermal energies, at around 1 MeV – 2 MeV (the evaporation peak), at around 100 MeV – 200 MeV (the quasi-elastic peak), and near the maximum incident particle energy. There is greater concern about high-energy neutron fields owing to the increasing number of high-energy accelerators in research and medicine and the special consideration given to the occupational exposure to cosmic radiation. In order to study the physics of neutron interactions in these applications, in particular concerning dosimetry, radiation protection monitoring of workplaces, and radiation effects in electronics, particularly those used in aircraft and in spacecraft, well-characterized neutron fields for high energies are needed.

In the present Report, EURADOS working group 11 presents the argument that well-characterized quasi-monoenergetic neutron (QMN) sources reaching into the energy domain above 20 MeV are needed. We present an overview of the existing facilities, discuss their advantages and disadvantages, and present a list of key factors that an ideal QMN source for dosimetry and spectrometry should offer. Two simulated high energy reference fields are also described.

The Report concludes that, out of the worldwide six QMN facilities currently in existence, all operate in sub-optimal conditions for dosimetry. Of the three facilities in Japan, one is at least temporarily out of action, and the only currently available QMN facility in Europe capable of operating at energies above 40 MeV, TSL in Uppsala Sweden, is threatened with shutdown in the immediate future. In Europe, a facility, NFS at GANIL, France, is currently under construction. NFS could deliver QMN beams up to about 30 MeV. It is, however, so far not clear if and when NFS will be able to offer QMN beams or operate with only so-called white neutron beams. It is likely that in about five years, QMN beams with energies above 40 MeV will be available only in South Africa and Japan, with none in Europe.

1. Introduction

Neutron sources are used and neutron radiation fields are generated in various scientific research areas and applications, for example in radiation therapy, in radionuclide production for medical applications, in material science studies, for the design of electronic components, in energy production, military activities, and in neutron radiography. High-energy neutrons are the dominant component of the prompt radiation field present outside the shielding of high-energy accelerators and are a significant component of the cosmic radiation fields in aircraft and in spacecraft. In radiotherapy using high-energy medical accelerators, high-energy neutrons are a secondary component of the fields in the beam delivery system and in the patient's body. The energy range of neutrons in these fields extends from thermal energies to several GeV, and the energy distributions of energy fluence generally have several regions of greater intensity: at thermal energies, at around 1 MeV – 2 MeV (the evaporation peak), at around 100 MeV – 200 MeV (the quasi-elastic peak), and near the maximum incident particle energy. High-energy neutron fields are gaining more attention owing to the increasing number of high-energy accelerators in research and medicine, and the special consideration given to the occupational exposure to cosmic radiation. In order to study the physics of neutron interactions in these applications, in particular concerning dosimetry, radiation protection monitoring of workplaces, and radiation effects in electronics, especially those used in aircraft and in spacecraft, well-characterized neutron fields for high energies are needed.

In medical applications using high-energy photons and ion beams for cancer treatment, one must consider the contribution of secondary neutrons to organs in the human body outside the target area. The neutron exposure of staff has to be included in the design and operation of the facility: the contribution of fast neutrons outside of the shielding was for a long time underestimated. In the environment outside the primary beam the neutron contribution to human radiation exposure can dominate, and neutrons with energies greater than 10 MeV – 20 MeV account for up to 50 % of the ambient dose equivalent.

The radiation field in aircraft and in space is a complex mixture of particles of galactic origin (GCR) and solar origin (SCR), as well as their secondary products produced in interactions with the atoms of the Earth's atmosphere, the material of the aircraft or spacecraft, the human body, and, for space, particles retained in the Earth's magnetosphere. Secondary neutrons are produced which cover the complete range from thermal neutrons up to neutrons of several GeV. For aircraft crew the neutrons can contribute up to 70 % of the total exposure. ICRP has given recommendations, and there is national legislation on the exposure of persons to cosmic radiation: millions of passengers are exposed in aircraft, and aircraft crew are among the most highly exposed radiation workers. There is concern about the radiation exposure of astronauts, a small group, but with special radiation protection procedures which differ significantly from those applied on Earth. The contribution of neutrons to the exposure of astronauts is between 10 % and 50 % of the total exposure. Dosimetry for exposures to cosmic radiation in aircraft is specified in ISO standards 20785-1 (2006), 20785-2 (2011), and 20785-3 (in press) and recommendations on exposure are given in ICRU Report 84 (2010).

There is still a lack of information on the biological effectiveness of high-energy neutrons and this is an area which calls for further research. The relative biological effectiveness of the different neutron energy regions to total biological detriment varies from relatively low for thermal and the 100 MeV – 200 MeV regions, to high for the evaporation region.

In order to make measurements of high-energy neutron fields, or for benchmark measurements of calculated fields, it is necessary to calibrate instruments in reference fields at energies from 20 MeV up to an energy approaching 1 GeV. There are ISO reference fields which extend up to 20 MeV (ISO 8529-1 (2001); ISO 8529-2 (2000); ISO 8529-3 (1998)) but not at higher energies. For the calibration of instrumentation, which includes the characterization of the response, neutrons of energies greater than 20 MeV are required.

Reference high-energy neutron fields, quasi-monoenergetic neutron (QMN) fields, are of importance, because they allow for detailed studies of energy dependent responses of both active and passive devices. QMN fields have been made available over recent years for energies up to several hundred MeV, each with its own characteristics, advantages and short-comings. Some of these facilities have been shut down. At some of the facilities which are currently in operation, efforts have been made to develop standard reference fields and to compare their characteristics. However, these efforts are still incomplete and, furthermore, it has become increasingly difficult to keep the current facilities in full operation. For the determination of the neutron response characteristics of devices at these higher energies, measurements may sometimes be made in mono–energetic proton beams in combination with calculations, or in broad energy distribution neutron fields, also in combination with calculations. Most instruments will require their responses to non-neutron components of the radiation field to be determined. This is of particular importance for space radiation.

In this Report, EURADOS working group 11 presents the argument that well-characterized reference quasi-monoenergetic neutron (QMN) sources with neutron energies above 20 MeV are needed. There are six QMN facilities currently in existence worldwide. These operate in less than optimal conditions, especially when seen from the viewpoint of dosimetry. Of the three facilities in Japan, one is at least temporarily out of action, and the only currently available QMN facility in Europe capable of operating at energies above 40 MeV, TSL in Uppsala Sweden, is threatened with shutdown in the immediate future. In Europe, one facility, NFS at GANIL, France, is under construction, but it will be restricted to energies below 40 MeV. It is likely that in about five years from now, QMN beams with energies above 40 MeV will be available only in South Africa and Japan, with none in Europe. The audience for this Report are scientists working in high-energy radiation fields; advisors to funding bodies for high-energy research; experts on radiation field standards; members and consultants to regulatory bodies; manufacturers of instruments for high-energy radiation fields; users of high-energy radiation fields; airlines, hospitals, space agencies, research institutions.

2. Quasi-monoenergetic neutron fields above 20 MeV

The quasi-monoenergetic neutron field facilities described in this section all make use of the ^{7}Li(p,n) reaction for neutron production. The resulting neutron energy distributions consist of a peak close to energy of the incoming proton and a broad and roughly even distribution down to zero energy. Examples are shown below. Each of these components generally contain about half the neutron intensity. The width of the QMN peak comes from two contributing factors: the energy loss of the primary beam in the Li target, and the fact that the ^{7}Li(p,$n_{0,1}$)^{7}Be reaction (Q = -1.644 MeV) reaches both the ground state of ^{7}Be(n_0) and the first excited state at 0.429 MeV (n_1). While the latter cannot be avoided, the former (the dominant contribution) can be reduced by suitable choice of Li target thickness at the expense of the neutron fluence rate (the thinner the target, the narrower the high-energy peak, the lower the neutron fluence rate). The width of the square distribution of the neutron peak energy given an incoming proton beam of 50 MeV and using a Li target of 4 mm thickness (giving an energy loss of about 2.3 MeV) is about 2.7 MeV. The resulting mean peak neutron energy would thus be 47.2 MeV, while the peak is, strictly speaking, a square distribution stretching from 45.70 MeV to 48.36 MeV. The figures below show, due to limited experimental resolution, a width that is wider than the true width. It is also normally assumed that the (p,n) reaction reaches the Be ground state and first excited state with equal probability.

The tail in the neutron energy distribution comes from break-up reactions and is reasonably well described using a phase-space distribution. A more detailed study of the shape of neutron energy spectra and a suggested systematic is given by Prokofiev et al., 2002. An overview on quasi-monoenergetic high-energy neutron standards above 20 MeV is given by Harano et al., 2011.

2.1 iThemba LABS, South Africa

Detailed information on the quasi-monoenergetic fields at the iThemba Laboratory for Accelerator Based Sciences (iThemba LABS) facility, Faure, near Cape Town (previously, the National Accelerator Centre) can be found in the papers by McMurray et al., 1993; Nolte et al., 2002; Nolte et al., 2007; and Mosconi et al., 2010. Five beams at neutron peak energies of about 35 MeV, 65 MeV, 97 MeV, 147 MeV and 197 MeV at 0° and 16° have been characterized by time-of-flight spectrometry, using a proton recoil telescope for the measurement of the fluence in the peak for the lowest energy and a ^{238}U fission chamber for the remaining energies. The relative fluence energy distribution was measured up to 70 MeV with a scintillation detector, and above this energy, by a combination of scintillation detector and fission chamber. For the 97 MeV beam, the full width half maximum of the peak is about 4 MeV, and the fraction of the total fluence within the peak is about 0.4 increasing to 0.5 at 197 MeV. For the higher energies, this fraction can be effectively increased to ~0.7 by using a difference method, subtracting the instrument response for the 16° beam from that at 0°. For the 16° beam, the QMN peak is greatly reduced but with much less reduction in the lower energy continuum. The beam metrology is traceable to national standards via the fluence and energy distributions made by PTB, Germany.

Figure 1 shows the layout of the iThemba LABS neutron vault. At the iThemba LABS facility one loads the targets from the vault requiring the passageway that causes the background problems indicated in the iThemba LABS Annual Report 2009. The beamline is 1.5 m from the ground and has about the same distance to the roof. Measurement can be made in 4° steps from 0° to 16°. Sample spectra are shown in Figures 2 and 3.

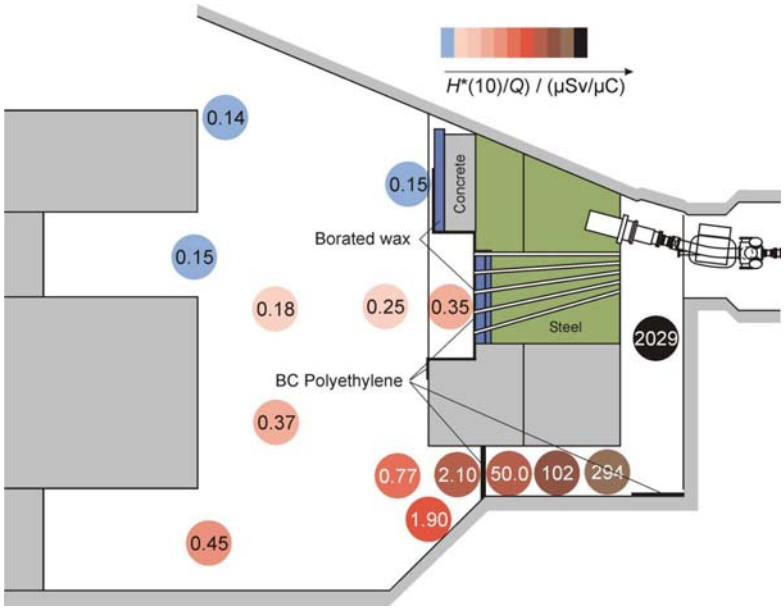

Figure 1: Ambient dose equivalent per beam charge (H^*/Q) in (μSv/μC) at several locations in the target room and in the experimental area of the iThemba LABS neutron beam facility. The ambient dose equivalent per charge in the direct neutron beam is about 6 μSv/μC. The energy of the proton beam incident on a thin Li target is 200 MeV.

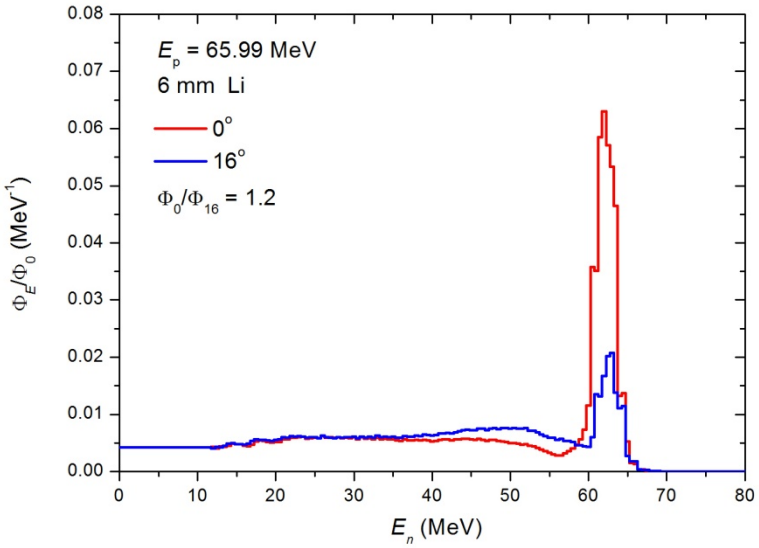

Figure 2: Neutron energy distributions of fluence at iThemba LABS for an incoming proton energy of 65.99 MeV and a Li target thickness of 6 mm. Energy distributions at two different angles are shown.

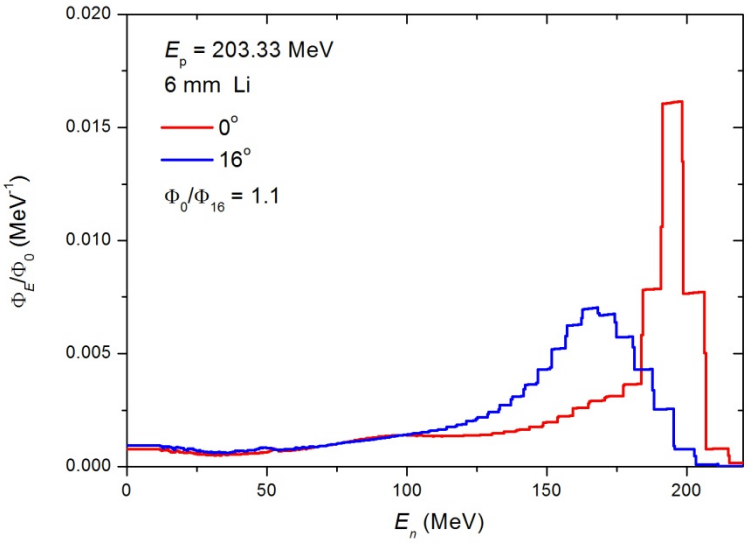

Figure 3: Neutron energy distributions of fluence at iThemba LABS for an incoming proton energy of 203.33 MeV and a Li target thickness of 6 mm. Energy distributions at two different angles are shown.

Measurements are usually carried out at an 8 m distance from the target. Energies available so far are from 66 MeV to 200 MeV. The beam is pulsed with 38 ns between pulses at 200 MeV and increases to 61 ns at 66 MeV. Currents of up to 700 nA can be used without pulse selector. Pulse selection is available as 1 in 3, 1 in 5, or 1 in 7, depending on the energy.

2.2 TSL, Sweden

A description of the neutron fields provided at the The Svedberg Laboratory (TSL) may be found in the paper by Prokofiev et al., 2007. A layout of the facility is shown in Figure 4. The beam is pulsed with 45 ns between pulses at 180 MeV, the pulse rate increases as the energy decreases. Below 100 MeV the proton current can reach 10 µA, while above 100 MeV the maximum current is about 300 nA. The average energies of the peaks of the fluence distributions for the neutron beams which can be provided range from 11 MeV to 175 MeV, with a full width half maximum of about 2 MeV – 5 MeV, depending on beam energy and the chosen Li target thickness. The neutron beam is monitored by means of a thin film breakdown counter (TFBC) and an ionization chamber monitor (ICM). A special feature of the facility is the availability of collimator openings ranging from 1 cm to 30 cm. Thus beam diameters of more than 1 m can be reached at the largest distance.

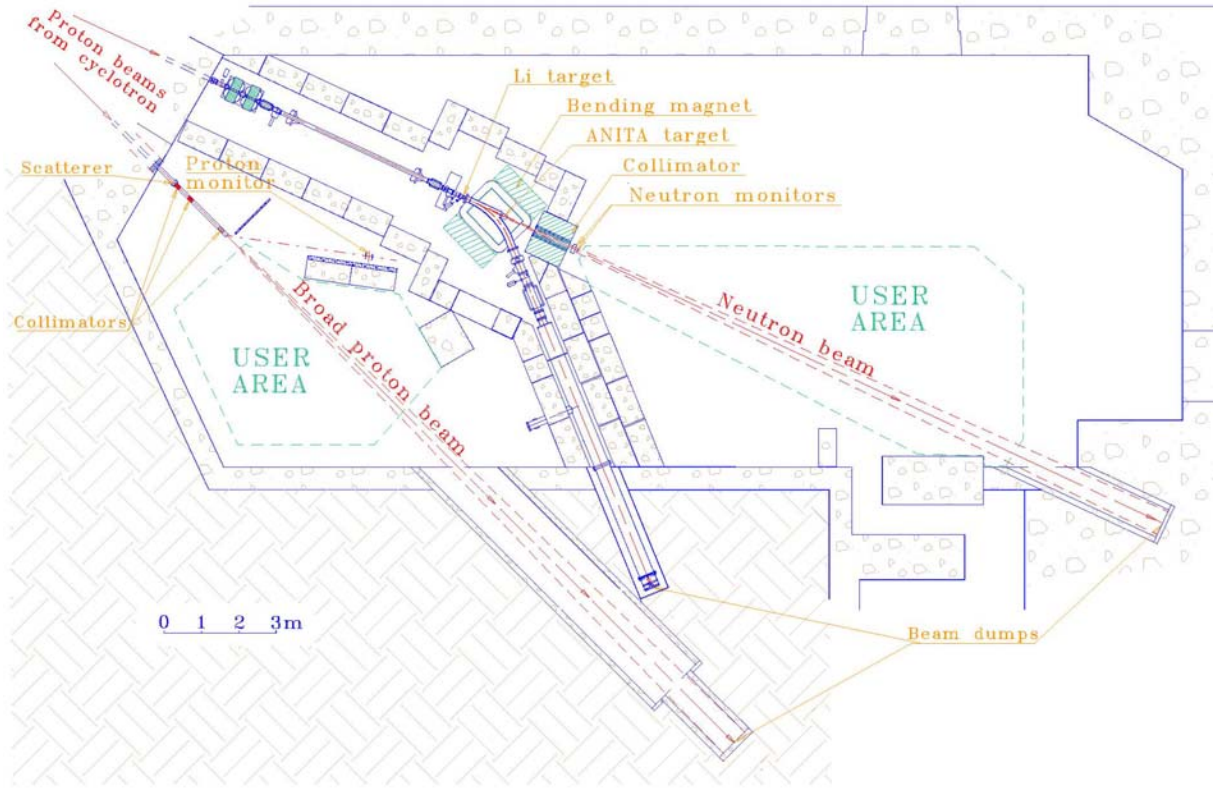

Figure 4: Layout of the TSL neutron beam facility (D-line).

There are some data on the neutron energy distribution of the lower-energy component, but only above about 5 MeV determined from both measurements and calculations. Examples of measured neutron energy distributions are shown in Figures 5 and 6. Below about 5 MeV, the fluence energy distributions (Φ_E) might be extrapolated to lower energies with Φ_E constant (Nolte et al., 2002). The ratio of peak fluence to total depends on peak energy, but is about 0.4. The peak neutron fluence rate reaches 10^6 cm^{-2} s^{-1} for proton energies below 100 MeV and 10^5 cm^{-2} s^{-1} for higher energies. The

uncertainty on the peak fluence is typically about 10 %. The uncertainties in the total fluences are estimated to be about 30 %, when the uncertainties in the energy distributions are taken into account. At present, the metrology of the fields is not traceable to any national standards.

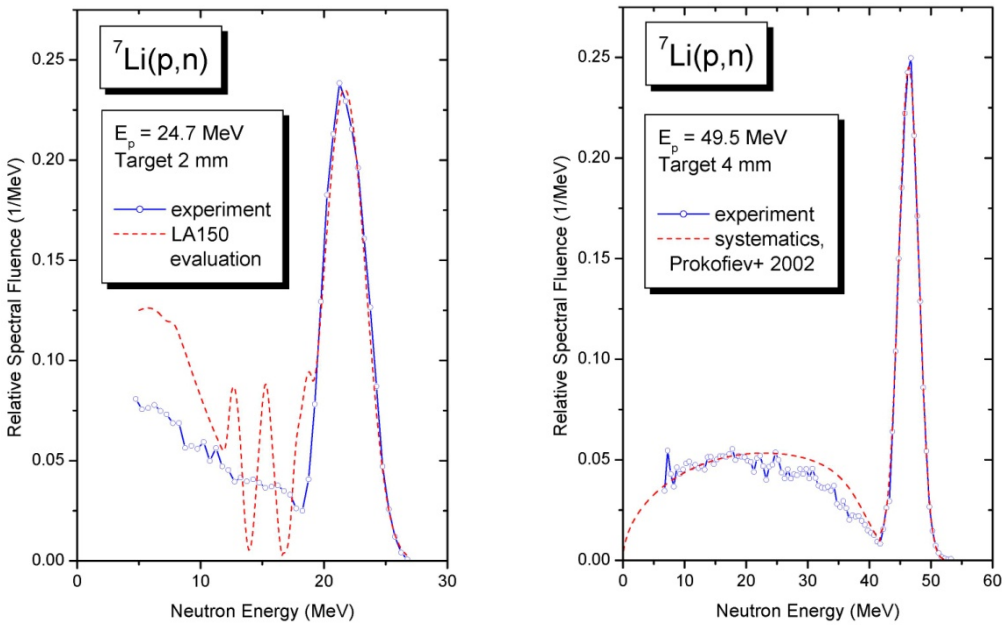

Figure 5: Neutron energy distributions of fluence as measured from elastic scattering using the proton recoil technique compared to the LA-150 evaluation and the systematics by Prokofiev. The latter have been folded with the experimental resolution to reproduce the peak width in the measurement.

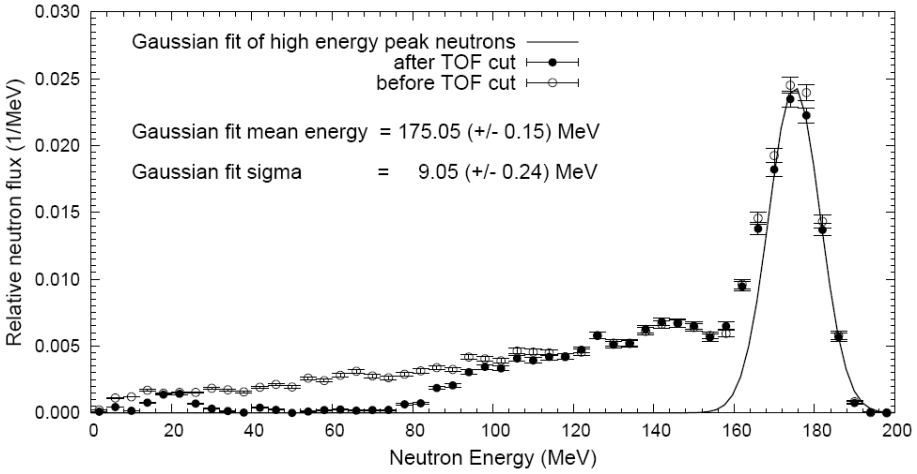

Figure 6: Relative neutron energy distributions at the maximum proton beam energy of TSL. The Li target thickness was 23.5 mm and the resulting neutron peak energy is 175 MeV. The measurement was done using the proton recoil technique. The filled dots indicate the effect of a TOF cut for the present experiment (Tippawan et al., 2011).

2.3 Facilities in Japan

2.3.1 Overview

In Japan, three cyclotron-based neutron fields over a wide energy range from 20 MeV to 400 MeV are available for various experiments such as characterization and development of radiation instruments, physics and chemistry research including cross section studies, shielding benchmark tests and quantification of electronic device errors.

These neutron fields are available at the Takasaki Ion Accelerators for Advanced Radiation Application (TIARA) in the Takasaki Advanced Radiation Research Institute (TARRI) of the Japan Atomic Energy Agency (JAEA), the Cyclotron and Radioisotope Center (CYRIC) of Tohoku University and the Research Center for Nuclear Physics (RCNP) of Osaka University. In all facilities, quasi-monoenergetic neutron beams are generated through the $^{7}Li(p,n)^{7}Be$ reaction.

2.3.2 TIARA

A field of quasi-monoenergetic neutrons for the energy range of 40 MeV to 90 MeV has been set up at TIARA (Baba et al., 1999). In this facility, accelerated protons from the AVF cyclotron are transported to a ^{7}Li disk. Protons passing through the target are bent into an iron dump with Faraday cup to capture the beam. The interval between beam pulses ranges from 45 ns to 90 ns, depending on the proton energy. In order to provide beam pulses spaced at intervals over 1 μs, a chopping system, consisting of two types of high voltage kickers, is installed in the cyclotron (Yokota et al., 1997). The Faraday cup and ^{238}U and ^{232}Th fission chambers around the target are used as beam monitors (Figure 7). Also, a thin plastic scintillation has recently been installed to monitor neutron beams at the collimator exit. The neutrons produced are guided to an experimental room through a collimator about 3 m thick. The dimensions of the room are 11 m wide, 19 m long, and 6 m high. The distance from the ^{7}Li target where measurements can be performed can be adjusted from 5 m to 18 m.

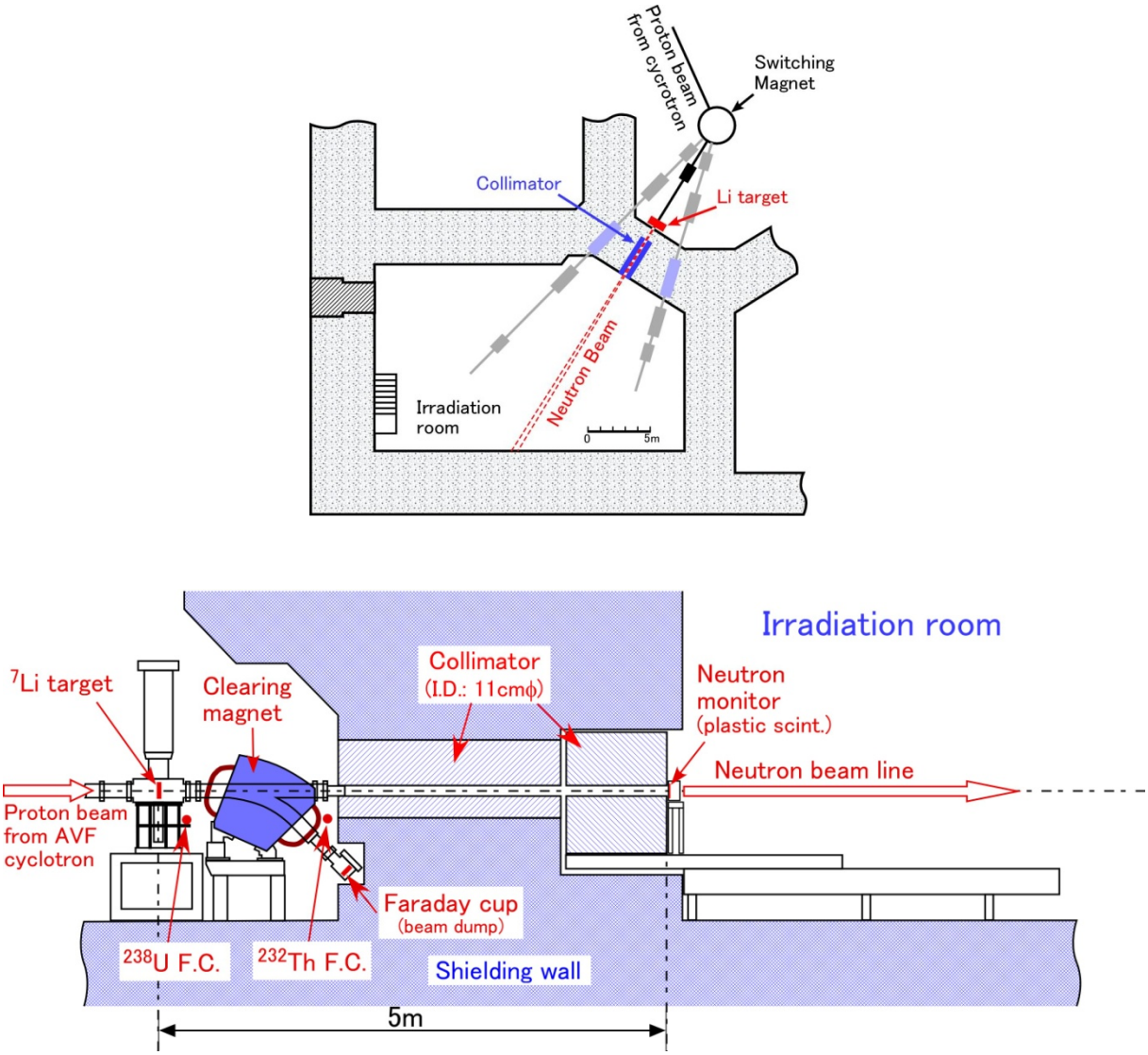

Figure 7: Illustration of the beamlines and instruments for neutron irradiation at TIARA. Top: drawing of the facility as seen from above; bottom: cut along the neutron beamline.

The uniformity across the central part of the irradiation area, with a diameter of about 90 % of the irradiated area, is within 3.5 %. Neutron beam profile, neutron energy distributions, and absolute neutron fluence were evaluated for the neutron fields with peak energies of 45 MeV, 60 MeV and 75 MeV (Shikaze et al., 2007, 2008, 2010). These characteristics are quite important for the reference calibration fields. The peak energy and energy distributions of the neutron beams (see Figure 8) have been measured by the time-of-flight (TOF) method using an organic liquid scintillation detector of which the response was well investigated by using the SCINFUL-QMD code (Satoh et al., 2002).

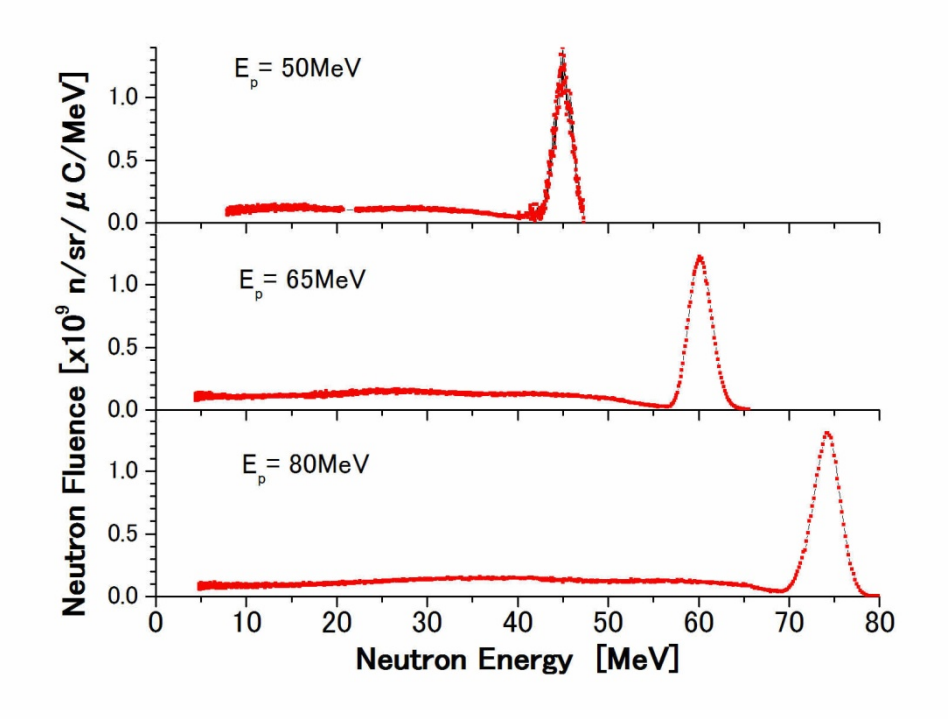

Figure 8: Neutron energy distributions per solid angle per electric charge measured with a 7.62 cm x 7.62 cm organic liquid scintillator by means of a time-of-flight method at TIARA. The neutrons were produced by the ^{7}Li(p,n) reaction using 50 MeV, 65 MeV and 80 MeV protons.

2.3.3 CYRIC

A high-intensity fast neutron beam facility in CYRIC has been developed at the straight beam line (32 course) from the K = 110 MeV AVF cyclotron since 2004 (Terakawa et al., 2002, Baba et al., 2007). This course is used for cross section measurements for nuclear physics, testing of semiconductors for single-event effects, and dosimetry development. The AVF cyclotron can provide proton beams with an energy ranging from 14 MeV to 80 MeV. Figure 9 shows a schematic view of the neutron source. The quasi-monoenergetic neutron beam is produced by using the $^{7}Li(p,n)^{7}Be$ reaction. The primary proton beam impinges onto the water-cooled production (Li) target. After penetrating the target, the proton beam is bent in the clearing magnet by 25° and stopped in a water-cooled beam dump which consists of a carbon block shielded by copper and iron blocks. The typical neutron beam intensity is about 10^{10} sr^{-1} s^{-1} μA^{-1} with a beam spread of about 5 % for the beam energy and ±2° for the horizontal and vertical directions. The neutron beam is collimated by 595 mm thick iron blocks and leading to sufficiently low background at the off-axis position. The available fluence rate of the neutron beam is about 10^{6} cm^{-2} s^{-1} μA^{-1} at the sample position, located at about 1.2 m downstream of the production target. The thermal neutron fluence rate at the sample position is about $2 \cdot 10^{4}$ cm^{-2} s^{-1}, which was measured by a foil activation method combined with an imaging plate.

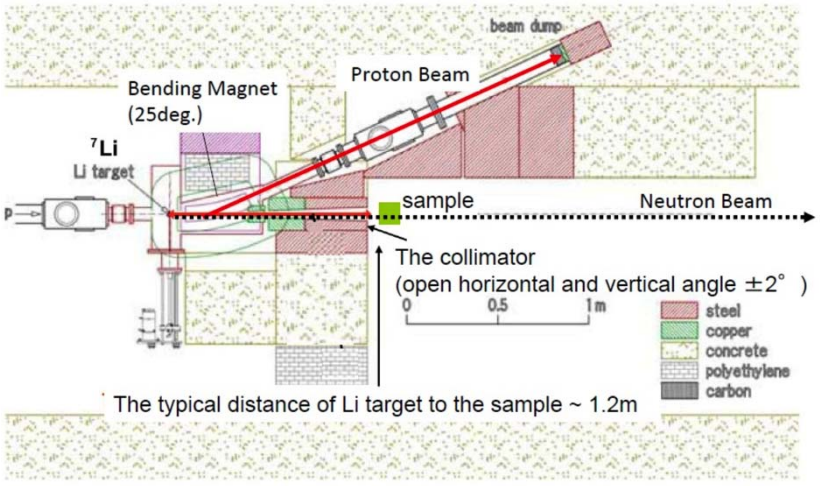

Figure 9: Schematic layout of the fast neutron beam facility CYRIC.

Figure 10 shows a typical energy distribution of the neutron beam at 65 MeV which was produced by 70 MeV protons. The thickness of the Li target was 9.1 mm. The energy distribution was measured by the time-of-flight (TOF) method 7.37 m downstream of the Li target. The energy spread of the neutron beam was 4 MeV which included the time spread of the primary beam of 1.6 ns, the energy loss due to the Li target thickness, etc. The ratio of the peak area to the total fast-neutron flux is about 0.4. The detection system for the fast neutrons consists of a liquid scintillator

of NE213 type with a diameter of 140 mm and a length of 100 mm, a 5 inch photomultiplier tube, HAMAMATSU H6527, which were assembled by OHYO-KOKEN cooperation, and a CAMAC data acquisition (DAQ) system. The irradiation room is a narrow room which size is 1.8 m (W) × 10 m (L) × 5 m (H). The irradiation sample can be placed at 1.2 m downstream the Li target, as shown in Figure 9. The size of the neutron beam is about 84 mm (horizontal) × 84 mm (vertical) at that point. The flux of the neutron beam can be varied from about a few hundred s^{-1} to $3{\cdot}10^{10}$ sr^{-1} s^{-1}. The largest accumulated fluence in one experiment was about $5{\cdot}10^{11}$ cm^{-2} for the practical irradiation time of 50 hours. The fluence rate of the neutron beam is monitored by the primary beam current in the beam dump and a NE102A plastic scintillator with a diameter of 100 mm and a thickness of 1 mm during the irradiation experiment. Users can control beam on/off via a LabVIEW program.

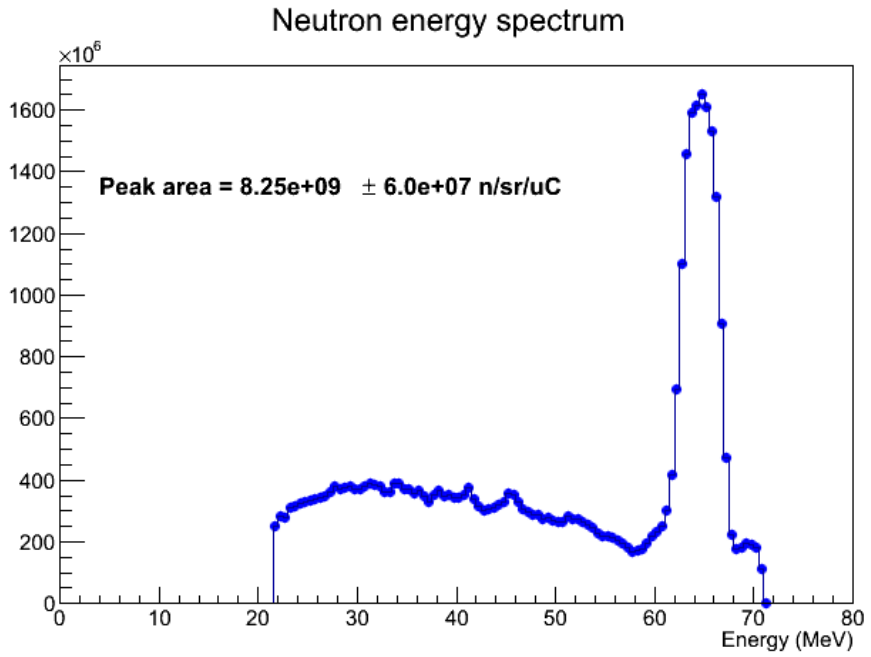

Figure 10: A typical energy distribution of the neutron beam at 65 MeV. Neutrons per solid angle per electric charge of a peak area from 58 MeV to 68 MeV is $8.25{\cdot}10^{9}$ sr^{-1} μC^{-1}. The ratio of the peak area to the total fast neutrons is about 0.4. The tail at around 70 MeV is attributed to the wrap around due to the cyclotron RF cycle.

2.3.4 RCNP

A quasi-monoenergetic neutron field for the energy range of 100 MeV to 400 MeV has been developed at the RCNP cyclotron facility of Osaka University. In this facility protons are accelerated up to 65 MeV using an AVF cyclotron and can be boosted up to 400 MeV in the Ring Cyclotron. The accelerated protons are transported to the experimental port and impinge on a 10 mm thick ^{7}Li target placed in a vacuum chamber. Protons passing through the target are swept out by the swinger magnet to the beam dump equipped with a Faraday cup current monitor. The experimental tunnel has a length of about 100 m (Figure 11), which enables precise measurements of energy distributions by the time-of-flight method (Taniguchi et al., 2007; Iwamoto et al., 2011). The potential as a high-energy neutron reference field has been investigated for proton beams with energies of 140 MeV, 250 MeV, 350 MeV and 392 MeV (Figure 12). The highest number of neutrons per solid angle per electric charge reaches $1.0 \cdot 10^{10}$ sr^{-1} μC^{-1} for 140 MeV to 392 MeV protons.

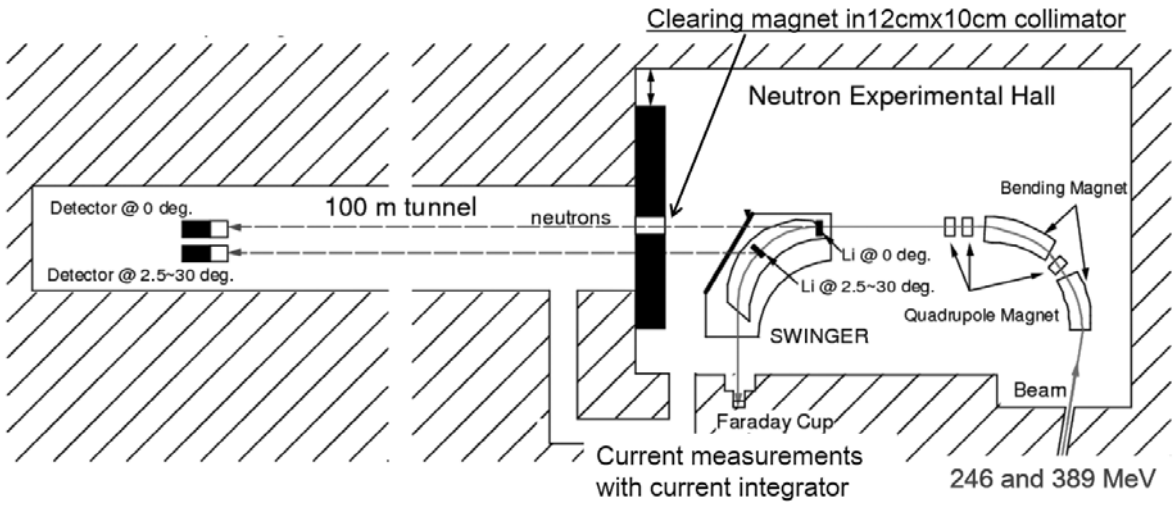

Figure 11: Illustration of the experimental set-up for neutron irradiation at RCNP.

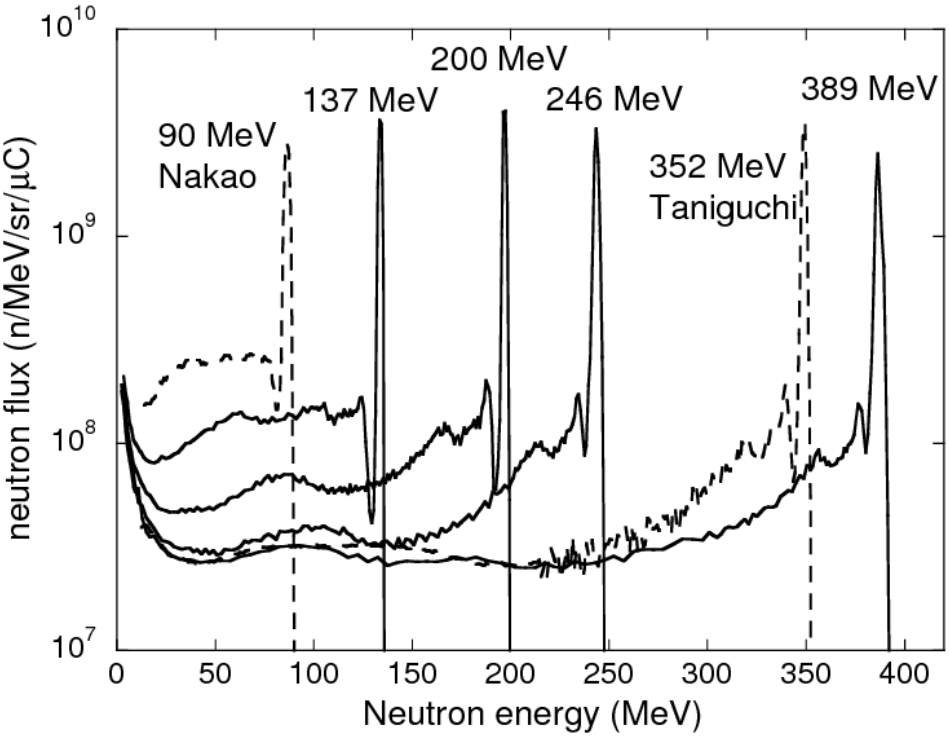

Figure 12: Neutron energy distribution per solid angle per electric charge for 137 MeV, 200 MeV, 246 MeV and 389 MeV produced by Li(p,xn) reaction at 0°; they are compared with the data obtained by Nakao et al., 1999, and Taniguchi et al., 2007.

Currently, the National Metrology Institute of Japan (NMIJ) in the National Institute of Advanced Industrial Science and Technology (AIST) is performing intensive studies for standardization of the quasi-monoenergetic neutron fields of TIARA in comparison with CYRIC and has also started characterization studies on the higher energy neutron field of RCNP (Harano et al., 2010).

2.4 NPI, Czech Republic

The Nuclear Physics Institute (NPI) at Řež, Czech Republic, can provide neutron beams with peak energies up to 36 MeV. Standards beams in MeV are 18, 21.6, 24.8, 27.6, 30.3, 32.9 and 35.6, respectively (Honusek et al., 2010). As at the other facilities, the neutron beam is produced from a ^{7}Li target. However, this facility differs in that the proton beam is not bent towards a beam dump but stopped in a carbon disc directly behind the lithium target (see Figure 13). This arrangement allows placing target samples at distances as close as 48 mm from the lithium target. Therefore, a neutron fluence rate of about 10^{9} cm^{-2} s^{-1} in the QMN peak at 30 MeV, can be achieved.

The energy distribution of the fluence rate at irradiation positions has been simulated using time-of-flight data from CYRIC that have been validated using the LA-150 library of cross section data with the transport Monte Carlo code MCNPX (Novák et al., 2010). The simulated energy distributions were compared to absolute measurements performed with a proton-recoil telescope technique.

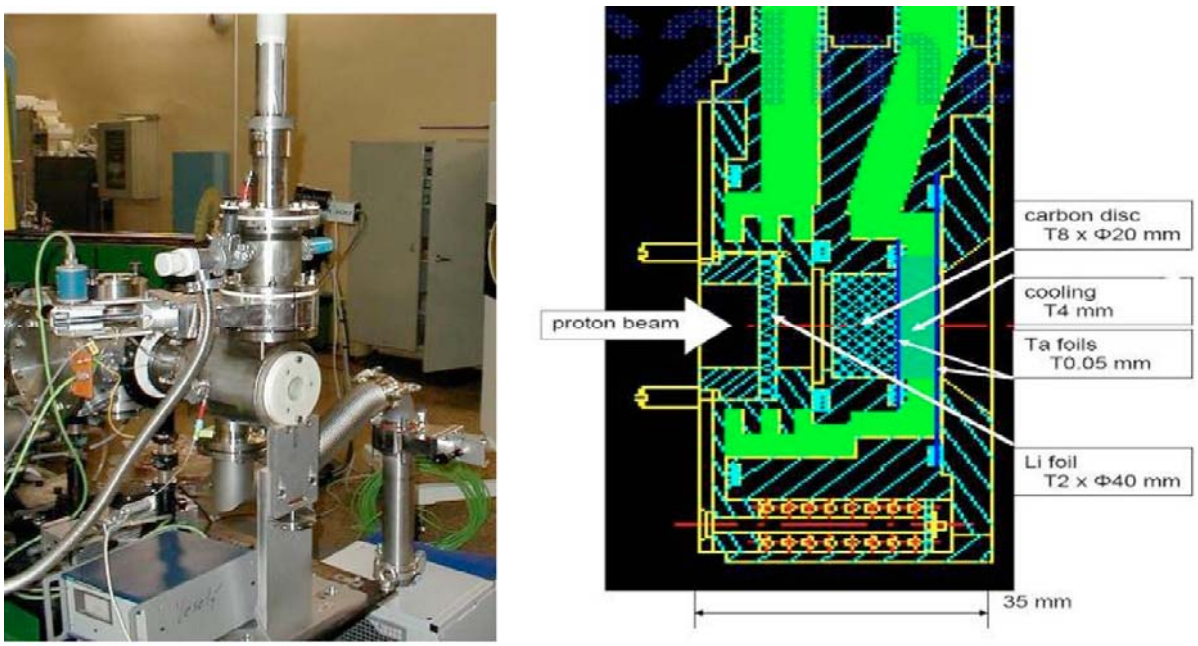

Figure 13: View of the target station of the NPI neutron source (left). Drawing of the reaction chamber (right). Figure taken from Honusek et al., 2010.

2.5 NFS, GANIL, France

A new facility that will offer both a white neutron energy spectrum and a QMN spectrum is currently under construction at GANIL in Caen, France. The facility is called Neutrons For Science (NFS) and is expected to deliver its first beams late 2014.

The neutron production targets at NFS will be located in a converter cave (see Figure 14). The beams are delivered to an experimental area which is separated by a 3 m thick concrete wall from the converter cave. Besides neutron production targets, the converter room will also offer irradiation set-ups for experiments needing the highest intensities. A bending magnet placed between the converter and the collimator entrance will clean the neutron beam from protons. A conical channel through the wall defines the neutron beam. The experimental area (25 m x 6 m) will allow performing time-of-flight measurements by using experimental set-ups at distances from 5 m up to 25 m from the neutron production point.

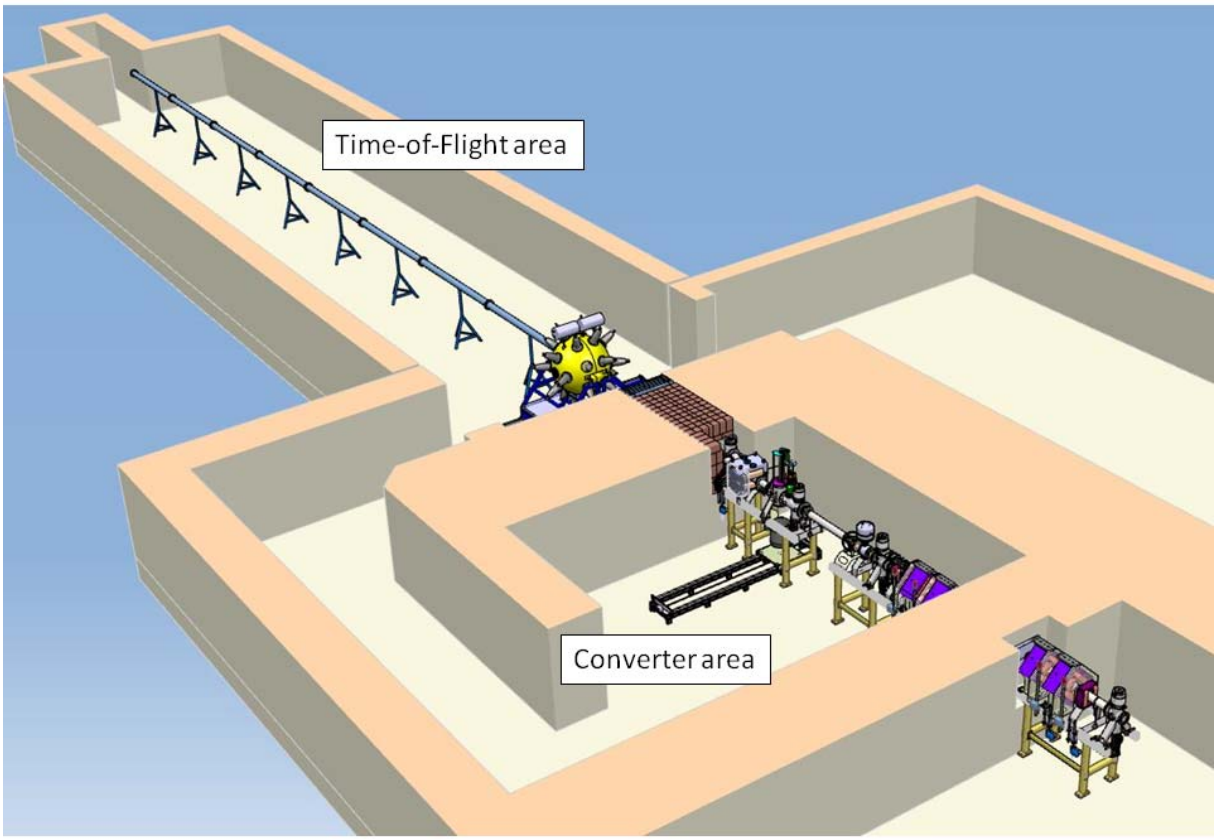

Figure 14: Schematic view of the NFS layout. The neutron production area (Converter area), and the experimental area (Time-of-Flight area) are shown. The beam from the LINAG enters from the lower right side.

The new Spiral 2 LINAG (LINear Accelerator of Ganil) will deliver pulsed proton and deuteron beams up to 33 MeV and 40 MeV respectively at a maximum intensity of 5 mA in pulses that are shorter than 1 ns. Two production modes will be used. The deuteron break-up reaction on a thick

converter made of carbon or beryllium generates neutrons with a continuous energy distribution. At 0°, the energy distribution extends up to 40 MeV with an average value of approximately 14 MeV. The ^{7}Li(p,n) reaction on a thin lithium target (1 mm to 3 mm of thickness) produces a QMN beam as shown in Figure 15.

Although the LINAG can deliver proton and deuteron beams with currents up to 5 mA, the ion beam intensity on the neutron production targets will be voluntarily limited to 50 µA. The reduced intensity means reduced wall thickness for radiation protection and reduced activation of the converter. It will also mean a manageable power distribution on the neutron production targets.

Furthermore, the LINAG beam frequency (88 MHz) is not optimized for time-of-flight measurements. In order to avoid wrap around effects, the neutron beam frequency must be reduced to below 1 MHz. Therefore, a fast beam-chopper downstream of the RFQ will select 1 over N bursts, with $N > 100$ corresponding to a maximum ion-beam intensity of 50 µA.

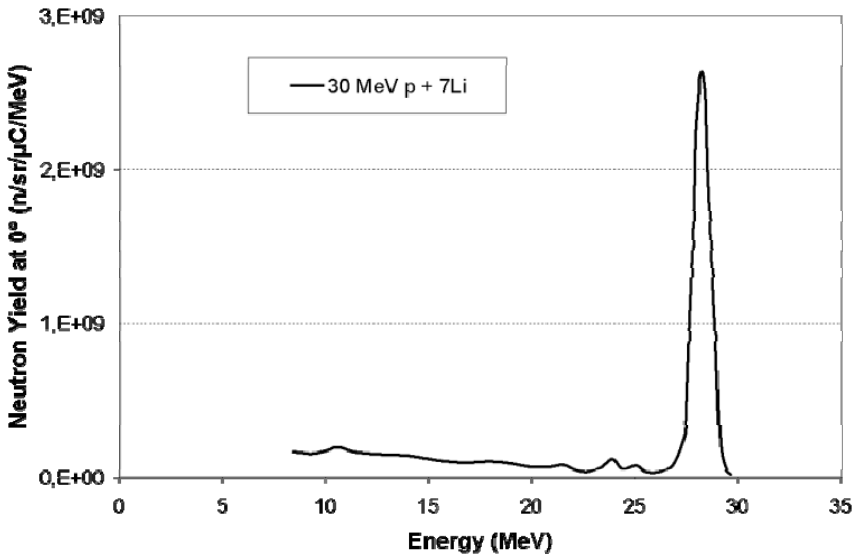

Figure 15: Calculated energy distribution of neutrons per solid angle per beam charge at 0° produced by the ^{7}Li(p,n) reaction on a thin lithium target at NFS.

3. Simulated workplace high-energy neutron fields

3.1 Medical and research facilities

There are workplace radiation fields with a high-energy neutron component in medical facilities and in fields near research accelerators. Neutrons are generated by reactions in the target, in target shielding, in collimators, in the patient or device being investigated, and in the room shielding. An example of such a neutron field for the characterization of measurements and calculations at GSI is shown in Figure 16. A benchmark exercise took place at this laboratory in July 2006, with the participation of fourteen research centres in the framework of the CONRAD project funded by the EU and coordinated by EURADOS. A beam of 400 MeV/u ^{12}C ions hit a thick graphite target, and measurements were carried out in the stray radiation field behind thick shielding representing a typical workplace field. Measurements with several Bonner Sphere Spectrometers were performed to characterise the field in the various positions, backed-up by extensive Monte Carlo simulations with two codes, FLUKA (Battistoni et al., 2007, Ferrari et al., 2005) and MCNPX (Hendricks et al., 2005). Several types of active detectors and passive dosimeters were intercompared. Mostly neutron measuring devices, as 90 % to 95 % of the ambient dose equivalent at the measurement positions was due to neutrons. However, various models of TEPC and other instruments capable of discriminating the low-LET from the high-LET component of the field were also employed (Rollet et al., 2009, Wiegel et al., 2009, Silari et al., 2009). Once properly characterized experimentally and by Monte Carlo simulations, such fields can in turn be used to check the response of instrumentation in broad neutron fields.

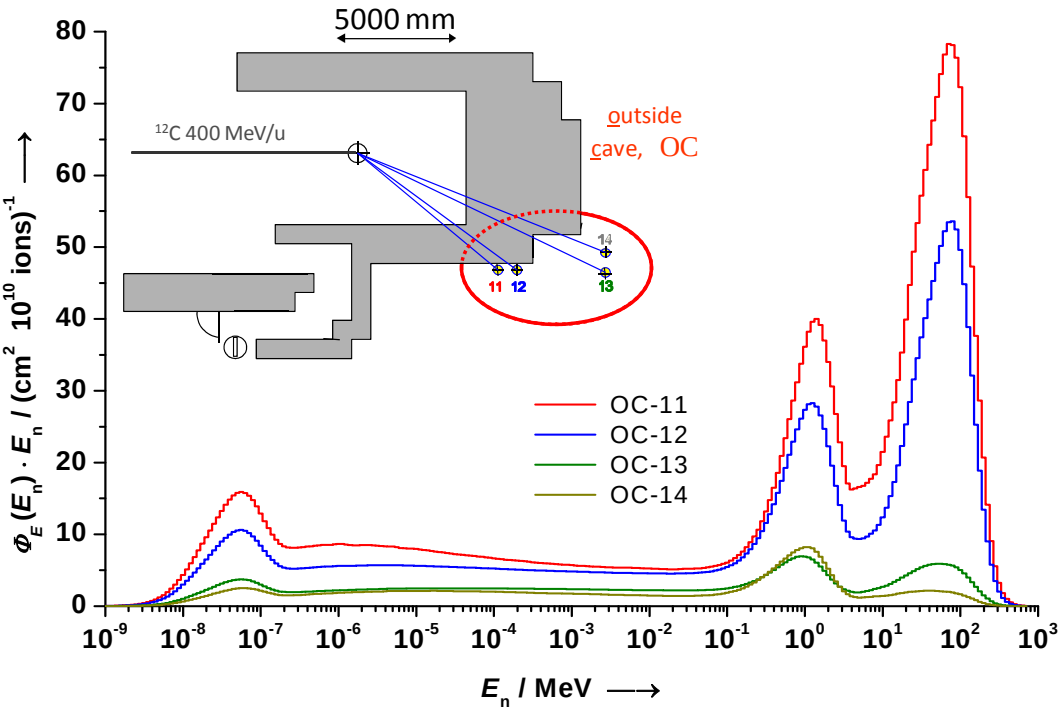

Figure 16: Measured neutron energy distributions of energy fluence outside a cave at GSI.

3.2 The CERN-EU high-energy Reference Field (CERF) facility

High-energy neutron fields are also produced by the interactions of cosmic radiation in the atmosphere, and of cosmic radiation with the spacecraft, its components, and crew. A facility to simulate this neutron component at CERN in Switzerland is the CERN-EU Reference Field (CERF) facility, providing since 1992 a few weeks of beam time per year. The field simulates closely the neutron field at commercial flight altitudes and in spacecraft (see Figure 17) (Mitaroff and Silari, 2002). It also provides a stray radiation field similar to those typically encountered around high-energy hadron accelerators. These radiation environments are dominated by neutrons with energy distributions ranging from thermal energies up to several GeV, but other components of the radiation field, mainly protons and photons, must also be considered when carrying out calibration of radiation detectors. In addition to the radiation field present behind thick shielding, high-energy particle cascades occurring close to the beam impact point are of frequent interest for radiation detector testing and material activation studies.

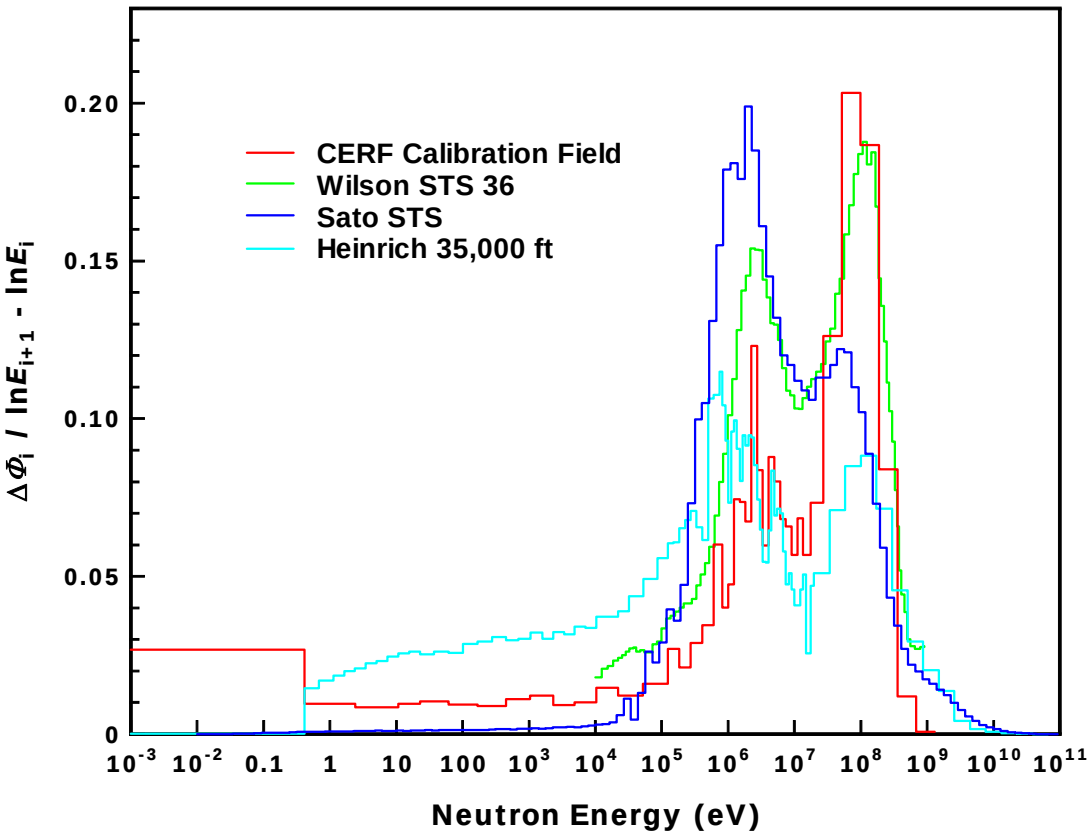

Figure 17: CERF calculated relative neutron energy distribution of energy fluence compared with those calculated for aircraft and spacecraft (Heinrich et al., 1999, Wilson et al., 2002, and Sato et al., 2006).

CERF is therefore suitable for testing and intercomparing radiation detectors (fixed monitors, hand-held instruments and personal dosimeters) routinely employed for operational radiation protection at particle accelerator facilities and for monitoring the cosmic ray fields on board aircraft and in space, as well as for in-field calibrations of instrumentation.

The reference radiation fields are produced by a 120 GeV/u hadron beam hitting a copper target, with several reference exposure locations available behind various types of shielding and around the target. The energy distributions of the particles at the various exposure locations were obtained by Monte Carlo simulations performed with the FLUKA code (Battistoni et al., 2007, Ferrari et al., 2005). Neutron fluence energy distributions on the concrete roof-shield, on the iron roof-shield and behind the 80 cm thick concrete lateral shield are plotted in Figure 18. The particle fluence energy distribution composition on the concrete roof-shield is shown in Figure 19. The neutron energy distribution on top of the concrete shield shows a marked high-energy neutron component resembling fairly closely the neutron field produced by cosmic rays at commercial flight altitudes. The fluence energy distribution outside the iron shield is rather dominated by neutrons in the 100 keV – 1 MeV range. Figure 20 shows the location inside the cave, with a superimposed dose map presenting the dose in Gy per primary particle hitting the target. The figure also shows the maximum dose rates and the particle fluence distributions for two typical irradiation locations inside the cave.

By adjusting the beam intensity on the target one can vary the dose-equivalent rate at the reference exposure locations. The maximum achievable dose-equivalent rates depend on various parameters linked to the SPS operation. In the past (with 2.6 s beam extraction time within an SPS cycle of 14.4 s, or 5.1 s spill within 16.8 s) maximum dose rates of up to 1 mSv/h on the iron roof-shield and up to 500 μSv/h on the 80 cm concrete roof or lateral shield were achievable. In recent years (with a much longer SPS cycle of about 45 s and a lower sharing of the beam towards the H6 beam line) the dose-equivalent rates have been almost a factor of 10 lower.

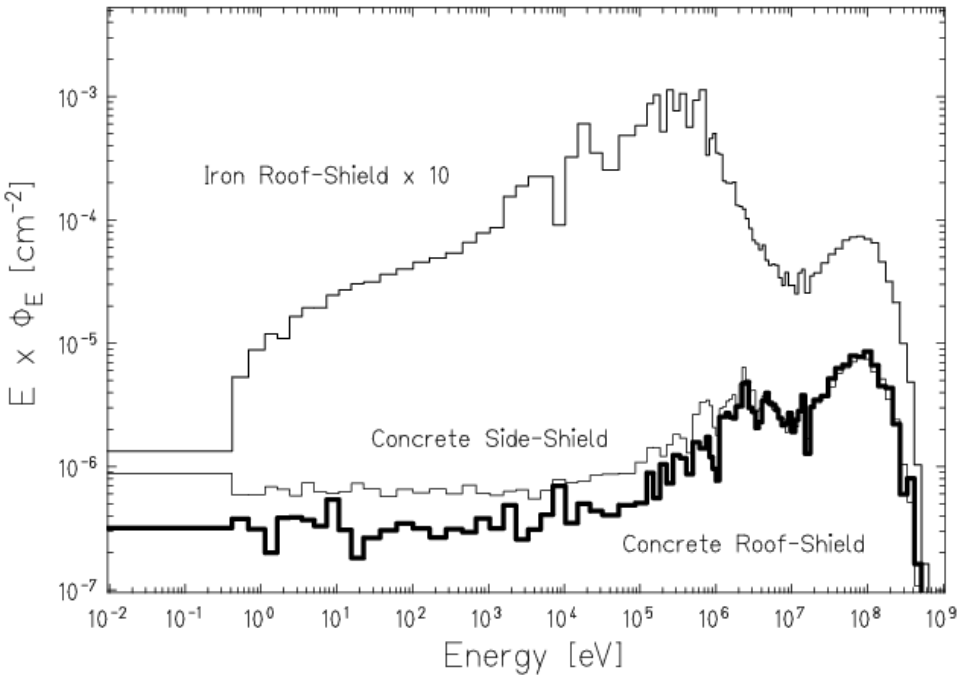

Figure 18: Neutron energy distributions of energy fluence on the concrete roof-shield, on the iron roof-shield and behind the 80 cm thick concrete side-shield (neutrons per primary beam particle incident on the copper target).

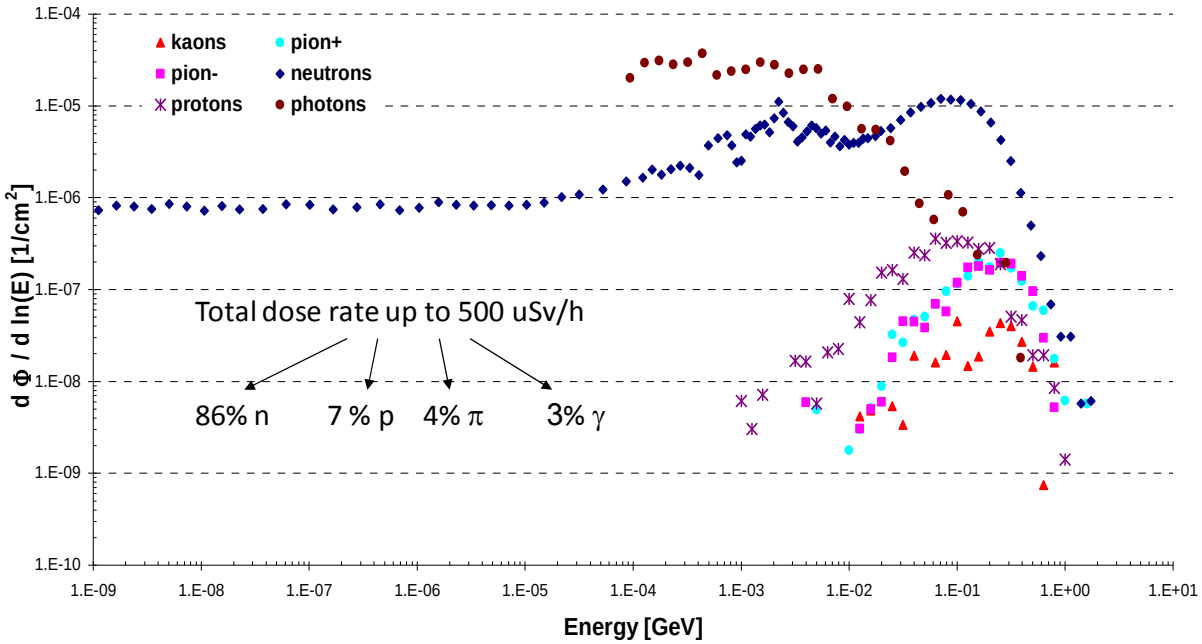

Figure 19: The composition of the energy distributions of particle energy fluence on the concrete roof-shield (particles per primary beam particle incident on the copper target).

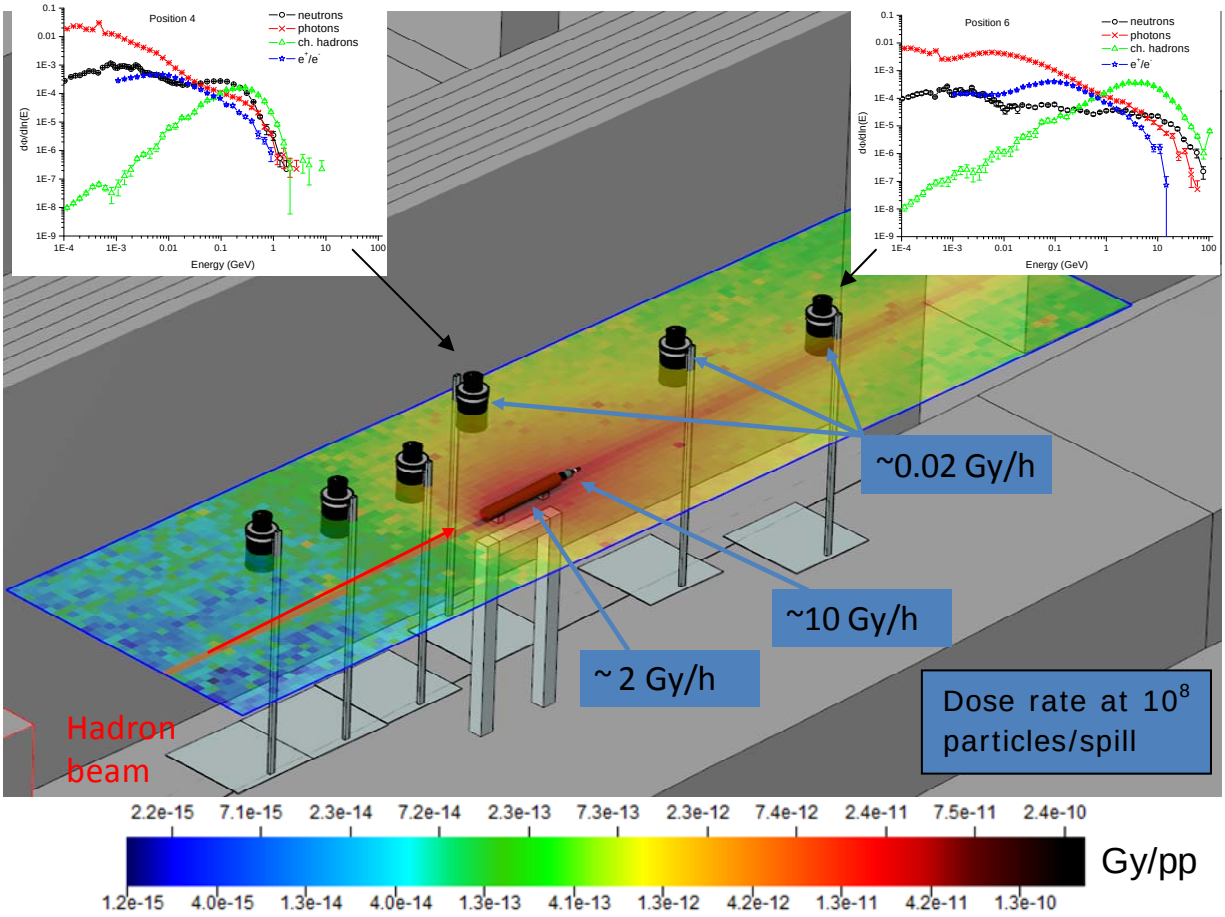

Figure 20: CERF target cave, superimposed by a dose map presenting the dose in Gy per primary particle hitting the target. The graphs on top of the picture show the particle fluence distribution at two measurement positions per primary particle impinging on the target.

Several measurement campaigns have taken place at CERF yearly starting in 1992. Many institutions from all over Europe, as well as all over the world have used the facility to test various types of passive and active detectors. Other experimental applications for which the facility has been used include tests related to the CERN LHC project, investigations of computer memory upsets and radiobiological studies. Several benchmark experiments for Monte Carlo based particle transport codes like FLUKA were also performed. A shielding experiment was performed to evaluate the attenuation length of iron for high-energy neutrons. The irradiation positions close to the target have also been used for material activation studies and high-level dosimetry calibrations, studies of detector responses of beam loss monitors and ionization chambers to mixed high-energy radiation fields.

4. Discussion and conclusions

Reliable radiation protection monitoring of workplaces at high-energy radiation fields in medical facilities, research accelerator environments, on-board aircraft, and in space, requires numerical simulations of an instrument's fluence response and its benchmarking to high-energy neutrons above 20 MeV. These benchmark measurements need careful calibration, traceability to national standards, determination of uncertainties, and intercomparisons of various instrument assemblies. To this end quasi-monoenergetic neutron reference fields (QMN), and more generally high-LET calibration fields, with good traceability are needed.

All six currently active facilities, and a planned future NFS facility, make use of the same nuclear reaction to produce the QMN beams, the $^{7}Li(p,n)^{7}Be$ reaction. It is therefore to be expected that similar experiences have been made at the various facilities. Generally speaking, none of the existing facilities were originally conceived for QMN applications, but mostly are adapted from an existing infrastructure at an accelerator laboratory. Several facilities suffer from too much background caused by scattered neutrons in a room not large enough for QMN measurements. A low background can only be achieved in a large irradiation hall provided with a raised floor, so that the neutron source and the detector under test can be located close to the centre of a large volume, as at various national metrology institute neutron irradiation facilities. Only a few have a path long enough to allow precise time-of-flight measurements. Some of the facilities report logistics problems, such as sub-optimal access to the target area and/or the experimental room, lack of a remote system for exchanging targets, or insufficient space provided to the users to set-up their experiment. In some cases the shielding between the target area and the experimental room is not efficient enough.

From the experience gained at the operational facilities described in this report, several conclusions regarding an optimized QMN reference field can be drawn. An ideal QMN facility should offer:

- quasi-monoenergetic neutron fields over a wide energy range (offering peak energies from about 20 MeV to several hundred MeV);
- well-characterized neutron energy distributions;
- a low, well characterized background.

To achieve this, several key factors are relevant:

- a stable short-pulsed proton beam of sufficient intensity;
- adjustable time between subsequent proton pulses (pulse selection/beam kicker);
- access to the neutron production room without a passage from the measurement area, possibly even complete remote control of target changes;
- several neutron beam lines at various angles (from 0° up to about 25°), this can facilitate the subtraction of the non-peak fluence;
- large measurement area/experimental hall to allow for usage of time-of-flight methods; suitable general working environment (office space, access to workshop, etc.);
- sunken floor and raised roof to minimize ambient background;
- provision of stable and reproducible high quality beams.

An additional desirable feature would be the option to switch to neutron fields to simulate a workplace field, for example an atmospheric-like neutron energy fluence distribution, to allow testing and intercomparison of instruments.

Besides these listed technical aspects, accessibility is an important feature for any user and, for several reasons, this is generally difficult for all the facilities. We note that three out of the six operating facilities are located in Japan, and one, iThemba LABS, in South Africa. Furthermore, owing to normal routine activities during weekdays, iThemba LABS only offers QMN beams during weekends. Finally, all the four mentioned facilities normally require a nuclear physics involvement in dosimetry and metrology for measurements which is often difficult to provide.

After the shut-down of the facility in Louvain-la-Neuve a few years ago, TSL in Sweden is the only European facility that offers beams with energies above 40 MeV. However a major task of TSL is the construction of a dedicated facility for proton cancer therapy, and lacking Government support, the TSL QMN is facing being closed down in the immediate future.

It is likely that no QMN beams with energies above 40 MeV will be available in Europe in the near future. There exists the need to make measurements, and to benchmark calculations, of the increasing number of high-energy neutron fields. It is an unfortunate situation if the calibration of instruments cannot be done in Europe. Therefore a new, dedicated, European reference QMN facility is required providing energies at least to 200 MeV.

Acknowledgements

The authors of this report are grateful for the help of Iva Ambrožová, Pavel Bém, Luke Hager, Yosuke Iwamoto, Xavier Ledoux, Tetsuro Matsumoto, Takashi Nakamura, Alexander Prokofiev, Yasuhiro Sakemi, and Yoshihiko Tanimura in its preparation.

References

Baba, M., Nauchi, Y., Iwasaki, T., Kiyosumi, T., Yoshioka, M., Matsuyama, S., Hirakawa, N., Nakamura, T., Tanaka, Su., Meigo, S., Nakashima, H., Tanaka, Sh., Nakao, N., 1999, *Characterization of 40-90 MeV ^{7}Li(p,n) neutron source at TIARA using a proton recoil telescope and a TOF Method*, Nucl. Instr. Meth. A 428, 454-465.

Baba, M., Okamura, H., Hagiwara, M., Itoga, T., Kamada, S., Yahagi, Y., Ibe, E., 2007, *Installation and application of an intense ^{7}Li(p,n) neutron source for 20–90 MeV region*, Radiat. Prot. Dosim. 126, 13-17.

Battistoni, G., Muraro, S., Sala, P.R., Cerutti, F., Ferrari, A., Roesler, S., Fassò, A., Ranft, J., 2007, *The FLUKA code: Description and benchmarking,* Proceedings of the Hadronic Shower Simulation Workshop 2006, Fermilab 6-8 September 2006, M. Albrow, R. Raja eds., AIP Conference Proceeding 896, 31-49.

Dublin Institute for Advanced Studies Report DIAS 99-9-1, 1999, *Study of radiation fields and dosimetry at aviation altitudes* EU contract number F14P-CT950011, Final report, January 1996-June 1999, Dublin Institute for Advanced Studies, Dublin, Ireland.

EURADOS/CERN Report CERN-2006-007, 2006, *Complex workplace radiation fields at European high-energy accelerators and thermonuclear fusion facilities* (CERN:Genève).

European Commission Radiation Protection No 140, 2004, *Cosmic Radiation Exposure of Aircraft Crew: Compilation of Measured and Calculated Data*, European Radiation Dosimetry Group WG5 (EC: Luxembourg).

European Commission Radiation Protection No 160, 2009, *Technical recommendations for monitoring individuals occupationally exposed to external radiation*, European Radiation Dosimetry Group WG2 (EC: Luxembourg)

Fassò, A., Ferrari, A., Ranft, J., Sala, P.R., 2005, *FLUKA: a Multi-Particle Transport Code*, CERN-2005-10, INFN/TC_05/11, SLAC-R-773.

Fassò, A., et al., 2003, *The Physics Models of FLUKA: Status and Recent Developments*, Computing in High Energy and Nuclear Physics 2003 Conference (CHEP2003), La Jolla, CA, USA, March 24-28, 2003, (paper MOMT005), eConf C0303241, arXiv:hep-ph/0306267.

Ferrari, A., Sala, P.R., Fassò, A., Ranft, J., 2005, *FLUKA: a multi-particle transport code*, CERN-2005-10, INFN/TC_05/11, SLAC-R-773.

Harano, H., Matsumoto, T., Tanimura, Y., Shikaze, Y., Baba, M., Nakamura T., 2010, *Monoenergetic and quasi-monoenergetic neutron reference fields in Japan*, Radiat. Meas. 45, 1076-1082.

Harano, H., Nolte, R., 2011, *Quasi-monoenergetic high-energy neutron standards above 20 MeV*, Metrologia 48, S292.

Heinrich, W., 1999, *private communication* (see also *Study of radiation fields and dosimetry at aviation altitudes,* EU contract number F14P-CT950011, Final report, January 1996-June 1999, Report DIAS 99-9-1, Dublin Institute for Advanced Studies, Dublin, Ireland (1999).

Hendricks, J.S., Mc Kinney, G.W., Waters, L.S., Roberts, T.L., Egdorf, H.W., Finch, J.P., Trellue, H.R., Pitcher, E.J., Mayo, D.R., Swinhoe, M.T., Tobin, S.J., Durkee, J.W., Gallmeier, F.X., David, J-C., Hamilton, W.B., Lebenhaft, J., 2005, *MCNP-X Extensions version 2.5.0*, LA-UR-05-2675.

Honusek, M., Bém, P., Fischer, U., Götz, M., Novák, J., Simakov, S.P., Šimečková, E., 2010, *The cross-section data from neutron activation experiments on niobium in the NPI p-7Li quasi-monoenergetic neutron field*, EPJ Web of Conferences, Volume 8, 07004, EFNUDAT – Measurements and Models of Nuclear Reactions.

International Commission on Radiological Protection, 2013, *Assessment of the Radiation Exposure of Astronauts in Space*, ICRP Publication in preparation, Ann. ICRP.

International Commission on Radiation Units and Measurements, 2001, *Determination of Operational Dose Equivalent Quantities for Neutrons,* ICRU Report 66 Journal of the ICRU 1 (3).

International Commission on Radiation Units and Measurements, 2010, *Reference Data for the Validation of Doses from Cosmic-Radiation Exposure of Aircraft Crew* ICRU Report 84 Journal of the ICRU 10 (2).

International Organization for Standardization, 1998, *Reference neutron radiations – Part 3: Calibration of area and personal dosemeters and determination of response as a function of energy and angle of incidence.* ISO 8529-3 (ISO: Geneva).

International Organization for Standardization, 2000, *Reference neutron radiations – Part 2: Calibration fundamentals related to the basic quantities characterizing the radiation field.* ISO 8529-2(ISO: Geneva).

International Organization for Standardization, 2001, *Reference neutron radiations – Part 1: Characteristics and methods of production* ISO 8529-1(ISO: Geneva).

International Organization for Standardization, 2006, *Dosimetry for exposures to cosmic radiation in civilian aircraft – Part 1: Conceptual basis for measurement* ISO 20785-1:2006 (ISO: Geneva).

International Organization for Standardization, 2006, *Reference radiation fields – Simulated workplace neutron fields – Part 1: Characteristics and methods of production.* ISO 12789-1: 2006 (ISO: Geneva).

International Organization for Standardization, 2007, *ISO/IEC Guide 99 International vocabulary of basic and general terms in metrology (VIM)*, (ISO: Geneva).

International Organization for Standardization, 2008, *Reference radiation fields – Simulated workplace neutron fields – Part 2: Calibration fundamentals related to the basic quantities.* ISO 12789-2:2008 (ISO: Geneva).

International Organization for Standardization, 2010, *Reference radiation fields for radiation protection – Definitions and fundamental concepts* ISO/DIS 29661 (ISO: Geneva).

International Organization for Standardization, 2011, *Dosimetry for exposures to cosmic radiation in civilian aircraft – Part 2: Characterization of instrument response* ISO 20785-2:2011 (ISO: Geneva).

International Organization for Standardization, in preparation, *Dosimetry for exposures to cosmic radiation in civilian aircraft – Part 3: Measurements at aviation altitudes* ISO 20785-3:20xx (ISO: Geneva).

iThemba LABS, 2009, *Annual Report 2009*, Published in March 2009 by iThemba LABS, PO Box 722, Somerset West 7129, South Africa.

Iwamoto, Y., Hagiwara, M., Satoh, D., Iwase, H., Yashima, H., Itoga, T., Sato, T., Nakane, Y., Nakashima, H., Sakamoto, Y., Matsumoto, T., Masuda, A., Nishiyama, J., Tamii, A., Hatanaka, K., Theis, C., Feldbaumer, E., Jaegerhofer, L., Pioch, C., Mares, V., and Nakamura, T., 2011, *Quasi-monoenergetic neutron energy spectra for 246 and 389 MeV ^{7}Li(p,n) reactions at angles from 0°to 30°*, Nucl. Instr. and Meth. A 629, 43-49.

Joint Committee for Guides in Metrology, 2008, *International vocabulary of metrology - Basic and general concepts and associated terms (VIM) JCGM 200*, (BIPM: 2008).

McMurray, W.R., Aschman, D.G., Bharuth-Ram, K., Fearick, R.W., 1993, *The Faure cyclotron neutron source and a particle spectrometer for neutron induced emission of charged particles at energies between 60 and 200 MeV*, Nucl. Instr. and Meth. A 329, 217.

Mitaroff, A., Silari, M., 2002, *The CERN-EU high-energy Reference Field (CERF) facility for dosimetry at commercial flight altitudes and in space*, Radiat. Prot. Dosim. 102, 7-22.

Mosconi, M., Musonza, E., Buffler, A., Nolte, R., Röttger, S., Smit., F.D., 2010, *Characterization of the High-Energy Neutron Beam Facility at iThemba LABS*, Rad. Meas. 45, 1342.

Nakao, N., Uwamino, Y., Nakamura, T., Shibata, T., Nakanishi, N., Takada, M., Kim, E., Kurosawa, T., 1999, *Development of a quasi-monoenergetic neutron field using ^{7}Li(p,n)7Be reaction in the 70-210 MeV energy range at RIKEN*, Nucl. Instr. and Meth. A 420, 218-231.

Nolte, R., Allie, M. S., Binns, P.J., Brooks, F.D., Buffler, A., Dangendorf, V., Meulders, J.P., Roos, F., Schumacher, H., Wiegel, B., 2002, *High-Energy neutron reference fields for the calibration of detectors used in neutron spectrometry*, Nucl. Instr. Meth. A 476, 369.

Nolte, R., Allie, M.S., Brooks, F.D., Buffler, A., Dangendorf, V., Meulders, J.P., Schuhmacher, H., Smit, F.D., Weierganz., M., 2007, *Cross Sections for Neutron-Induced Fission of ^{235}U, ^{238}U, ^{209}Bi, and ^{nat}Pb in the energy range from 33 to 200 MeV measured relative to n-p scattering*, Nucl. Sci. and Engin. : 156, 197–210.

Novák, J., Bém, P., Fischer, U., Götz, M., Honusek, M., Simakov, S.P., Šimečková, E., Štefánik, M., 2010, *Spectral flux of the p-^{7}Li(C) Q-M neutron source measured by proton recoil telescope*, EPJ Web of Conferences, Volume 8, 06001, EFNUDAT – Measurements and Models of Nuclear Reactions.

Pelliccioni, M. 2000, *Overview of fluence-to-effective dose and fluence-to-ambient dose equivalent conversion coefficients for high energy radiation calculated using the FLUKA code*, Radiat. Prot. Dosim. 88, 279–297.

Prokofiev, A., Chadwick, M., Mashnik, S., Olsson, N., Waters, L., 2002, *Development and Validation of the ^{7}Li(p,n) Nuclear Data Library and Its Application in Monitoring of Intermediate Energy Neutrons*, J. Nucl. Sci. Technol., Suppl. 2, 112.

Prokofiev, A.V., Blomgren, J., Byström, O., Ekström, C., Pomp, S., Tippawan, U., Ziemann, V., Österlund, M., 2007, *The TSL Neutron Beam Facility*, Radiat. Prot. Dosim. 126, 18-22.

Rollet, S., et al., 2009, *Intercomparison of radiation protection devices in a high-energy stray neutron field, Part I: Monte Carlo simulations*, Radiat. Meas. 44, 649-659.

Sato,T., Niita, K., Iwase, H., Nakashima, H., Yamaguchi, Y., Sihver, L., 2006, *Applicability of particle and heavy ion transport code PHITS to shielding design of spacecrafts*, Radiat. Meas, 41, (9-10), 1142-1146.

Satoh, D., Kunieda, S., Iwamoto, Y., Shigyo, N., Ishibashi, K., 2002, *Development of SCINFUL-QMD code to calculate the neutron detection efficiencies for liquid organic scintillator up to 3 GeV*, J. Nucl. Sci. Technol., Suppl. 2, 657-660.

Shikaze, Y., Tanimura, Y., Saegusa, J., Tsutsumi, M., Yamaguchi, Y., Uchita, Y., 2007, *Investigation of properties of the TIARA neutron beam facility of importance for calibration applications*, Radiat. Prot. Dosim. 126, 163-167.

Shikaze, Y., Tanimura, Y., Saegusa, J., Tsutsumi, M., Shimizu, S., Yoshizawa, M., Yamaguchi, Y., 2008, *Development of the Neutron Calibration Fields using Accelerators at FRS and TIARA of JAEA*, J. Nucl. Sci. Technol.,, Suppl. 5, 209-212.

Shikaze, Y., Tanimura, Y., Saegusa, J., Tsutsumi, M., Yamaguchi, Y., 2010, *Development of highly efficient proton recoil counter telescopefor absolute measurement of neutron fluences in quasi-monoenergetic neutron calibration fields of high energy*, Nucl. Instr. Meth. A 615, 211-219.

Silari, M. et al, 2009, *Intercomparison of radiation protection devices in a high-energy stray neutron field. Part III: instrument response*, Radiat. Meas. 44, 673-691.

Takada, M., Yajima, K., Yasuda, H., Sato, T., Nakamura, T., 2010, *Measurement of atmospheric neutron and photon energy spectra at aviation altitudes using a phoswich-type neutron detector*, J. Nucl. Sci. Technol. 47, 932-944.

Taniguchi, S., Nakao, N., Nakamura, T., Yashima, H., Iwamoto, Y., Satoh, D., Nakane, Y., Nakashima, H., Itoga, T., Tamii, A., and Hatanaka, K., 2007, *Development of a quasi-monoenergetic neutron field using the $^{7}Li(p,n)^{7}Be$ reaction in the energy range from 250 to 390 MeV at RCNP*, Radiat. Prot. Dosim. 126, 23-27.

Terakawa, A., Suzuki, H., Kumagai, K., Kikuchi, Y., Uekusa, T., Uemori, T., Fujisawa, H., Sugimoto, N., Itoh, K., Baba, M., Orihara, H., Maeda, K., 2002, *New fast neutron time-of-flight facilities at CYRIC*, Nucl. Instr. Meth. Phys. Res. A 491, 419-425.

Tippawan, U., et al., 2011, *Light-ion Production in 175 MeV Neutron-induced Reactions on Oxygen*, J. Korean Phys. Soc. 59(2), 1979.

Wiegel B., et al., 2009, *Intercomparison of radiation protection devices in a high-energy stray neutron field Part II: Bonner sphere spectrometry*, Radiation Measurements 44, 660-672.

Wilson, J.W., 2002, *Private communication*.

Yokota, W., Fukuda, M., Okumura, S., Arakawa, K., Nakamura, Y., Nara, T., Agematsu, T., Ishibori, I., 1997, *Performance and operation of a beam chopping system for a cyclotron with multiturn extraction*, Rev. Sci. Instrum. 68, 1714-1719.

Appendix A: Fact sheet about QMN facilities

The following table summarizes key features of the 6 currently available facilities and one facility currently under construction. A more detailed description is given in section 2 and in the references.

Facility	**Energy range [MeV]**	**Peak neutron fluence rate at standard irradiation position [$cm^{-2}s^{-1}$]**	**Beam angle relative to primary beam**	**Remarks**
iThemba[a]	35 – 200	10^4	0°, 4°, 8°, 12°, 16°	
TSL[b]	11 – 175	10^6 for E_p < 100 MeV 10^5 for E_p > 100 MeV	0°	large experimental area
TIARA[c]	40-90	10^4	0°	large irradiation room
CYRIC[d]	20-90	10^6	0°	
RCNP[e]	100 - 400	10^5	0° - 30°	up to 100 m ToF
NPI[f]	18 – 36	Up to 10^9	0°	Standard irradiation very close to source
NFS[g]	20 – 33	n.a. yet	0°	Start late 2014

[a] Contact iThemba LABS: www.tlabs.ac.za. Owing to standard commercial operations during weekdays, the facility is available only during weekends for physics experiments.

[b] Contact TSL: www.tsl.uu.se. Beamtime requests are submitted to a PAC. Nevertheless, the user has, even for approved projects, to secure funding for paying the beamtime from other sources, e.g., EU infrastructure projects such as ERINDA or CHANDA. Due to proton therapy treatments, TSL normally runs at a proton beam energy of 180 MeV during three out of four weeks. Beam sharing with therapy is enabled in these weeks during daytime. In the remaining week the other energies are available according to the users' needs.

[c] Contact TIARA: http://www.taka.jaea.go.jp/tiara/j661/riyoutebiki/f_0103.htm (in Japanese). To apply, it is best to first contact a Japanese researcher or engineer who will be able to support your experiments.

[d] Contact CYRIC: http://www.cyric.tohoku.ac.jp/english/contact/index.html. To apply, it is best to first contact a Japanese researcher or engineer who will be able to support your experiments.

Facility	Energy range [MeV]	Info on time structure
iThemba[a]	35 – 200	Duration of proton pulse about 1 ns (FWHM). Pulsed beam with 61 ns between pulses at 66 MeV, and 38 ns at 200 MeV. Available pulse selection is 1 in 3, 1 in 5, or 1 in 7, depending on the beam energy.
TSL[b]	11 – 175	For E_p < 100 MeV: CW mode; RF is beam energy dependent. At E_p = 98 MeV the time between pulses is about 58 ns. For E_p > 100 MeV: FM mode; variable macro cycle; typical cycle length 2.5 ms; beam extraction typically during 800 µs per macro cycle; RF energy dependent; at E_p = 180 MeV time between pulses is about 45 ns .
TIARA[c]	40-90	Duration of proton pulse 1.5 ns to 2 ns (FWHM). Time between pulses varies from about 45 ns to several hundred ns. Repetition rate of the beam may be reduced down to 3.3 MHz (beam chopper)
CYRIC[d]	20-90	Duration of proton pulse 1.5 ns to 2 ns (FWHM). Beam pulse frequency is 18.92 MHz.
RCNP[e]	100 - 400	Time between pulses: 56 ns – 167 ns (6 MHz - 18 MHz): 86 ns between pulses @ 140 MeV (11.642 MHz) 75 ns between pulses @ 200 MeV (13.376 MHz) 69 ns between pulses @ 250 MeV (14.496 MHz) 60 ns between pulses @ 392 MeV (16.645 MHz). Pulse selection with beam chopper: 1/5, 1/7, 1/9.
NPI[f]	18 – 36	E_p = 20 MeV: pulse width 5.9 ns (FWHM), time between pulses 50.4 ns. E_p = 37 MeV: pulse width 5.2 ns (FWHM), time between pulses 38.6 ns.
NFS[g]	20 – 33	Pulse width less than 1 ns; time between pulses 1.1 µs.

[e] Contact RCNP: http://www.rcnp.osaka-u.ac.jp/eng/access/index.html. To apply, it is best to first contact a Japanese researcher or engineer who will be able to support your experiments.

[f] Contact NPI: Nuclear Physics Institute v.v.i., 25068 Rez, Czech Republic

[g] Contact NFS: www.ganil-spiral2.eu/spiral2-us. The facility is currently under construction. First beam expected for late 2014. Initially only white beams will be available. The QMN source for which the design values are given in this table will be implemented later.

Appendix B: Calibration of high-energy neutron fields

B.1 High-energy neutron fields

Neutron radiation fields play an important role in a large variety of applications, ranging from the medical area and dosimetry, to radiation effects in electronics in aircraft and spacecraft, neutron radiography, and energy production. In order to study the nuclear physics of neutron interactions in these applications, in particular concerning dosimetry and radiation protection monitoring of workplaces, well characterized neutron fields over a wide range of energies are needed. The neutron radiation fields near high-energy accelerators, in aircraft, and in space, have energies that extend to several GeV. In most cases, the particle fluence energy and angle response characteristics of an instrument are simulated by computer calculation. The simulated instrument response must be benchmarked in reference radiation fields.

The measurement of the neutron field at medical facilities, at high-energy accelerators, in aircraft, and in spacecraft, is a complex problem and requires:

- information on the radiation field;
- a decision about the field components to be measured or estimated;
- a characterization/calibration of the measurement devices or instrument assemblies;
- knowledge about the pulse rate/dose rate response;
- a measurement model;
- traceability of the response characterization and calibration;
- estimate of uncertainties;
- intercomparisons of measurement devices or instrument assemblies.

One approach to classify a complex radiation field is to separate the field into its neutron and non-neutron components. This approach is based on the detection technique applied since many measurement systems are sensitive or not sensitive to neutron radiation. Another approach is to divide the radiation field into energy deposition by low LET (< 10 keV/µm) and by high LET (> 10 keV/µm) components. This definition is based on the dependence of the quality factor on LET, which is equal to unity below 10 keV/µm. The energy deposition by low LET component comprises the following components: directly ionizing electrons, positrons and muons; secondary electrons from photon interactions; most of the energy deposition by directly ionizing interactions of protons; part of the energy deposition by secondary particles from strong interactions of protons and neutrons. The high LET component is from cosmic radiation primaries and fragments at high aviation altitudes and in spacecraft (in commercial aircraft at cruise altitudes, most of them are already fragmented or absorbed), and relatively short range secondary particles from strong interactions of protons and neutrons. There are similarities between the neutron- and high LET component, and the non-neutron- and low LET component. However for thermal and epithermal neutrons, and at neutron energies above 20 MeV, the neutrons produce, in addition to the high-LET component, a contribution below 10 keV/µm. This can affect the interpretation of results from TEPCs. Whichever approach is adopted, it is essential to determine the response of an instrument to neutrons, including the response to high-energy neutrons above 20 MeV.

For the monitoring of workplaces on the Earth's surface, the assessments of effective dose and equivalent doses are by the determination of personal dose equivalents; by the determination of ambient dose equivalent and occupancy factors; by the determination of the particle type, fluence energy and direction distributions together with occupancy and calculations; or by direct

calculations. These procedures are discussed in detail in a recent EURADOS WG2 Report 160 (EC, (2009)).

For the procedures for monitoring in aircraft the assessed doses are mainly based on the calculation of effective dose, with benchmark measurements of ambient dose equivalent. More information on this is in the EURADOS WG5 Report 140 (EC (2004)) and ICRU Report 84 (ICRU 2010)).

Operational radiation protection for astronauts in space, however, differs significantly from those requirements for external radiation exposure on Earth. The detriment from the radiation fields in spacecraft is assessed by a combination of calculations and measurements, and, to a lesser extent, occupancy. A discussion of radiation protection in space is given in an ICRP Report currently in preparation (2013).

The present report summarizes the characteristics of QMN facilities and tries to draw conclusions from the collected operational experience of these facilities. The result of this report is a number of recommendations, or rather a wish-list, for future QMN facilities.

B.2 Instruments and calibration procedure

B.2.1 Instruments for calibration

The types of detectors that can be used for measurements of neutron fluence, absorbed dose and its distribution in terms of LET, event size, or other weighting factors, or, with the application of conversion coefficients, in terms of ambient dose equivalent or personal dose equivalent, can be categorized as active or passive. Instruments intended to measure only the neutron component can also be sensitive to other particles, and their response to these particles must be determined. In some instances, a combined instrument system is installed to monitor ambient dose equivalent rates from several particles.

Active devices will include the following: tissue equivalent proportional counters (TEPC); neutron solid state energy deposition spectrometers; recombination chambers; large volume organic scintillators; moderate-and-capture devices employing a thermal-neutron detector surrounded by an hydrogenous moderator with an increased response for high-energy neutrons obtained by neutron scattering using high atomic number materials such as copper, lead or tungsten; multi-sphere neutron spectrometers.

Passive devices include the following: plastic nuclear etched track detectors and nuclear emulsions; fission foil detectors; superheated emulsion neutron detectors (neutron bubble detectors); real-time electronic personal dosimeters, most of which use silicon-based detectors; multi-detector spectrometers using different types of nuclear track and fission foil detectors.

Calibration might also be needed of instruments which are not intended for the measurement of neutrons, but to determine their neutron response. These might include: ionization chambers; Geiger Müller counters; luminescence detectors (TL, OSL, RPL); direct ion storage dosimeters.

For high-energy accelerators and aircraft, the dose quantity usually monitored is ambient dose equivalent. The conversion coefficients from fluence to ambient dose equivalent used are those of Pelliccioni (Pelliccioni, 2000).

For measurements in spacecraft, the preferred dose quantity for recording is the radiation quality weighted absorbed dose to an organ or tissue. Measurements are of fluence and fluence rate, with

information on the energy and direction distribution, or of absorbed dose, or radiation weighted absorbed dose, to a small element of tissue at the location of the instrument. The dose quantity monitored depends partly on whether it is for area monitoring or used as a personal dosimeter. For further discussion, see ICRP Report in preparation (2013).

B.2.2 Calibration procedures

Calibration [ISO VIM; JCGM 200] is an operation that, under specified conditions, in a first step establishes a relation between the quantity values with measurement uncertainties provided by measurement standards and corresponding indications by the instrument with associated measurement uncertainties and, in a second step, uses this information to establish a relation for obtaining a measurement result from an indication (instrument reading). A calibration may be expressed by a statement, calibration function, calibration diagram, calibration curve, or calibration table. In some cases it may consist of an additive or multiplicative correction of the indication with associated uncertainty. Calibration should not be confused with adjustment of a measuring system, often mistakenly called 'self-calibration', nor with verification of calibration. Often, the first step alone in the above definition is perceived as being calibration. The determination of the calibration coefficient function should be performed at a constant fluence and fluence rate. In the scope of the calibration of an instrument, the conditions, for example fluence, fluence rate, the axis of rotation, for which the calibration coefficient function was determined, have to be specified.

The instrument to be calibrated should include additional equipment which forms part of the instrument assembly which may be irradiated in actual measurements, e.g. for personal dosimeters this will include a phantom. The reference point of the instrument shall be positioned at the point of test at which the fluence is determined. For a personal dosimeter, this reference point is normally taken as being on the front surface of the phantom (but see ISO 12789-2:2008). The angle of incidence should be determined. The axis of rotation passes through the reference point of the instrument. The calibration is intended to be carried out under reference conditions or standard test conditions (see ISO/FDIS 29661:2012). The effects of any differences shall be considered in the uncertainty statement.

Where an instrument consists of more than one detector or more than one signal channel, the result of any algorithm to calculate the measured value is to be treated as the instrument indication in all determinations of calibration coefficient or response. The equation is useful for the determination of the uncertainty budget according to ISO/IEC Guide 98-3, "Guide to the Expression of Uncertainty in Measurement (GUM)". Whether the indication shall be corrected depends on the level of accuracy required.

For QMN, the radiation field at the point of test has a number of components in addition to the peak neutron energies. The non-peak components can contribute up to 70 % or 80 % of the fluence. These components will include the energy and direction distributions of the field generated by multiple scattering from the instrument assembly and the phantom if used. (See ISO standards ISO 12789-1:2008, ISO 12789-2:2008.) For the determination of the instrument response to the characteristic QMN neutron energy, the zero indication of the instrument needs to be calculated taking into account all other field components from the target as well as that scattered by the floor and walls of the laboratory, in a complex way. For some instruments the peak component can be separated by TOF techniques. In some QMN facilities, a separate beam configuration can enable partial determination of the non-peak component. The contribution of non-peak components to the instrument response characteristics can be evaluated by subtraction

methods for the non-peak signals. The evaluation of the instrument response characteristics to the peak energies will involve detailed calculations of the QMN radiation field at the point of test and an evaluation of the instrument responses for the non-peak energy and direction distributions. In general, the response characteristics of the instruments for high-energy neutron measurements should be determined by a combination of measurements and calculations. By Monte Carlo or other simulations, the response of an instrument can be determined in terms of neutron fluence, its energy distribution, and angle dependence. The simulated instrument response must be benchmarked in reference radiation fields. The correct characterization of the measuring assembly is essential, both to the field component to be measured and to any other component, together with an assessment of the uncertainty.

In routine dosimetry, two types of reference calibrations are important. The first type is the reference calibration in reference radiation fields, as described here, which are traceable to National Metrology Institutes (NMI), the aim of which is to obtain an absolute reference calibration factor or absolute reference calibration coefficient for the instrument. All instruments should have periodic laboratory reference calibrations, typically at intervals of about one to two years, or as required by the regulations. It might be necessary to confirm the stability of the dosimetric performance of the instrument at more frequent intervals. The second type is an internal calibration to normalize the response of all the instruments to a reference value which is given by a fixed procedure, for example using an internal calibration. This allows for the variations in sensitivity of instruments within a batch, or the variation with time of a single detector, for example. This procedure determines an individual normalization factor, or individual calibration factor. Periodic repeated internal calibrations are of particular importance for passive (solid state) personal dosimeters to adjust the normalization /calibration factors for changes due to repeated use, or to confirm that their performance has not changed. A suggested frequency is every 10 uses or every 2 years, whichever occurs first.

B.2.3 Measurements

A set of measurements establishes the relationship between the indication and the measured quantity value of an instrument using the calibration coefficient function of the instrument. The measured quantity value is for the measuring instrument under the reference conditions. The measured quantity value can also be expressed in terms of the response function (or matrix of responses). The reference conditions are those defined conditions under which the calibration is performed and are valid. Ideally, all response measurements might be performed for conditions that are similar to those in the occupational fields, otherwise the instrument indication must be corrected for all quantities of significant influence.

In the case of workplace fields, it is necessary to apply a correction factor or folded response for the energy and direction distribution of the field. Knowledge of these distributions at the measurement site is required. These distributions are folded with the calibration coefficient or response matrices or respective correction factors. One then obtains a single field-specific correction factor, or a single field-specific calibration coefficient or responses for measurements. Alternatively a field-specific calibration coefficient can be established directly or by some other means. The correction factor might include a field specific value to consider for deficiencies of the instrument or of the measurement process, resulting in an improvement of the accuracy of the dose assessment.

For measurements in aircraft this same correction factor might, in some instances, be applied for the range of flight altitude, geomagnetic latitude and solar modulation for which measurements are being made.

For further information on instruments and calibration for high-energy neutrons, the reader can refer to ISO 20785-1:2006; ISO 12789-1:2008; ISO 12789-2:2008; ISO/FDIS 29661:2012; EURADOS/CERN Report CERN-2006-007; ICRU Report 66.